

H4. SMR/1247
Lecture Note: 22

**WORKSHOP ON PHYSICS OF
MESOSPHERE-STRATOSPHERE-TROPOSPHERE
INTERACTIONS WITH SPECIAL EMPHASIS ON MST
RADAR TECHNIQUES**

(13 - 24 November 2000)

**THE PHYSICS OF
FORMATION OF ANISOTROPIC TURBULENCE**

Prof. W. K. Hocking

Dept. of Physics
University of Western Ontario
London, Ontario
CANADA

THE PHYSICS OF
FORMATION OF
ANISOTROPIC TURBULENCE



A quantitative measure of the degree of anisotropy of turbulence in terms of atmospheric parameters, with particular relevance to radar studies

W. K. Hocking and A. M. Hamza

Department of Physics, University of Western Ontario, London, Ontario N6A 3K7, Canada

(Received in final form 22 February 1996; accepted 26 April 1996)

Abstract—Anisotropic turbulence and specular reflectors have both been invoked to explain aspect-sensitive radar scatter from the atmosphere. However, conclusions about the dominant type of scatter are usually based on qualitative arguments, and can tend to be somewhat subjective. In this article, we develop a quantitative relation between the degree of anisotropy of turbulence and prevailing atmospheric conditions. This relation is useful in determining whether any particular observation of ‘specularity’ really can be ascribed to anisotropic atmospheric turbulence, or whether a ‘specular reflection’ process is in effect.
 © 1997 Elsevier Science Ltd

1. INTRODUCTION

‘Aspect sensitivity’ in radar experiments refers to the feature of preferential scatter of radio signals from overhead rather than from off-vertical angles. It is often (but not always) found that the signal received when the bore of a radar beam points directly overhead exceeds that received when an off-vertical beam is used. This characteristic is evident throughout the middle and lower atmosphere — at VHF (Very High Frequencies) in the stratosphere and troposphere, and at VHF, HF (High Frequencies) and MF (Medium Frequencies) in the mesosphere.

The history of observations of aspect-sensitive scatterers in the atmosphere is a very old and continuing one. There have been two main schools of thought concerning these scatterers. Some believe that the aspect sensitivity is indicative of horizontally stratified and extended ‘specular reflectors’ in the atmosphere. Others have advocated that the aspect sensitivity can be explained solely on the basis of anisotropic turbulence. One of the main problems has been that there is no quantitative theory that describes the limits to anisotropy which may be caused by turbulence. Some earlier experimental reports simply classified the scatterers as ‘specular’ and ‘isotropic’ (e.g. Gage and Green, 1978; Röttger and Liu, 1978; Hocking, 1979; Fukao *et al.*, 1979). Other studies presented measurements of the back-scattered power as a function of beam tilt angle (e.g. Lindner, 1975a, 1975b; Vincent and Belrose, 1978; Tsuda *et al.*, 1986). Subsequent studies attempted to quantify the degree of back-

scatter by representing the fall-off as a function of angle by some mathematical function; examples included Gaussian and exponential functions (e.g. Lindner, 1975a, 1975b; Vincent and Belrose, 1978; Waterman *et al.*, 1985). Various variations on simple measurements of power as a function of angle were also employed to further investigate this phenomenon (e.g. Röttger and Vincent, 1978; Woodman and Chu, 1989; Hocking *et al.*, 1990 amongst others). The most common parameterization has been to represent the power as a function of angle by a form proportional to $\exp\{-\theta^2/\theta_s^2\}$, where θ_s has been called the ‘aspect-sensitivity’ factor. The above references are not a complete set, but are adequate to establish the main features related to aspect-sensitivity studies: a more complete bibliography of studies related to this aspect sensitivity dependence can be found in Lesicar *et al.* (1994).

With the notable exceptions of Briggs and Vincent (1973) and Vincent (1973), few attempts were made prior to 1984 to relate these measurements and parameterizations to any features of the scattering entities themselves. However, in the 1980s efforts were finally successful in relating aspect-sensitivity measurements to quantities like the degree of anisotropy of the scatterers. These theoretical developments included ones by Doviak and Zrnic (1984) and Hocking (1987, 1989). The relation between the aspect sensitivity of the scattered radiation and the average shapes of the scattering entities is now fairly well understood. Experimental studies have been carried out which util-

ize these theoretical developments (e.g. Reid, 1990), including extensive multi-station climatologies reported by Lesicar and Hocking (1992) and Lesicar *et al.* (1994).

A major remaining problem is to determine what actually causes the anisotropy of the scatterers. Whilst we can now easily determine the degree of anisotropy, it is still not possible to decide if this anisotropy has been caused by turbulence, or (as is often claimed) whether other forces are at work which cause anisotropy which is much more pronounced than turbulence can produce alone (i.e. specularly). Discussions about the types of non-turbulent 'specular reflectors' which have been envisaged can be found in articles by Hocking and Röttger (1983), Hocking (1987, 1989), Hocking *et al.* (1991), Woodman and Chu (1989), and Reid (1990). We do not intend to discuss these mechanisms further here; we rather concentrate on obtaining a better feel for the level of anisotropy induced by turbulence.

In the following sections, we develop a simple expression which places limits on the degree of anisotropy which can reasonably be expected because of turbulence. The theory examines how wind-shear will act to distort initially isotropic eddies. It is thus most relevant at scales within the inertial range of turbulence where normal Kolmogoroff theory predicts that, in the absence of external distorting effects, the scales should normally tend towards isotropic (e.g. Bradshaw, 1975), irrespective of any initial anisotropy at the generating scales. We note that the theory may have deficiencies at the largest scales if those larger scales are produced anisotropically in the first place, but our purpose here is to apply our results to radar backscatter. Since such backscatter usually comes from scales within the inertial range, the theory is perfectly adequate for our purposes.

2. THEORY

Consider a scatterer of size l . Then the mean square diameter of such an eddy will be approximately $l^2 \sim (Kt)$, where t is the time since the eddy was 'created', and K is a (scale-dependent) diffusion coefficient. The scale dependence arises because diffusion within the eddy takes place because of the motions of even smaller eddies which are embedded inside it, and the nett diffusion is the cumulative effect of all such smaller eddies. By dimensional considerations, $K \sim lv$, where v is a typical velocity associated with movement within the eddy (typically considered to be comparable with the speed of rotation of a particle towards the perimeter of the eddy) and if we let the turbulent energy dissipation rate ϵ be $\sim v^2/t \sim v^3/l$, then $K \sim l^{4/3}\epsilon^{1/3}$. Substitution for K in the equation $l^2 \sim Kt$ therefore gives

$$l^2 \sim \beta \epsilon t^3, \quad (1)$$

where β is a dimensionless constant of order unity. This is a well known relation first noted by Batchelor (1950). Other derivations include that by Weinstock (1978), who obtained a value for β of order 0.5. Nevertheless, we will consider β to simply be of order 1 for the time being – we will see that our subsequent anisotropy formulae are in fact only weakly dependent on the actual value of β .

Now consider an idealized small, initially isotropic eddy in the presence of a mean wind shear, as shown in Fig. 1(a). We consider the eddy to be initially a spheroid, which may distort to become an ellipsoid as time progresses. For purposes of illustration (though we note that this condition is not mandatory for our general discussion), we consider that the eddy has a Gaussian variation in density across a section through its centre, superimposed upon a much larger mean

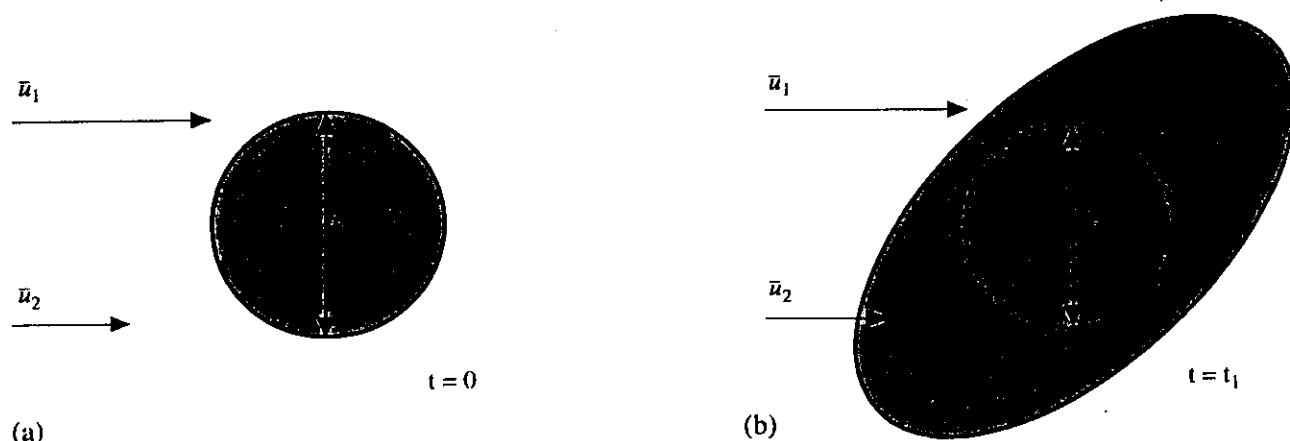


Fig. 1. An illustration of the nature of an eddy stretching in the presence of a wind shear.

background. This Gaussian perturbation from the mean may in fact be either positive or negative (i.e. the eddy could have either slightly higher density or slightly lower density than the surrounding atmosphere in which it is embedded). Such an eddy is represented in Fig. 1(a). The solid lines in that figure represent isopleths (contours) on a two-dimensional slice through the eddy along which the density perturbation is equal to the root-mean-square perturbation for the whole eddy.

We should note here that the concept of using different sized eddies as a representation of the turbulent density field is not at odds with the classical approach of representing the field as a power spectrum; De Wolf (1983) has shown the equivalence of the two approaches. However, for our derivations which follow, the eddy-like representation is much better suited, and we will not utilize the spectral approach until later in the article.

Let the initial diameter of the isotropic eddy be l_1 . The eddy will diffuse apart as time progresses, but will also be stretched horizontally by the wind shear. It will also gradually destroy itself during this process, and the energy it contains will cascade to smaller eddies, but we are most interested in this initial period of diffusive expansion. After time t , the vertical extent (vertical scale) of the eddy will be given by l_z , where

$$l_z^2 \sim \beta \epsilon t^3 + l_1^2. \quad (2)$$

Since the eddy was considered small at time $t = 0$, and we expect the degree of anisotropy to grow larger as the eddy evolves, we can neglect the small l_1 term, at least to first order, to give

$$l_z \sim \sqrt{(\beta \epsilon t^3)}. \quad (3)$$

We now turn to the horizontal stretching of the eddy, and begin by recognizing that it will have two terms. There will be firstly the diffusion term, as also occurs vertically, but there will also be a horizontal stretching caused by the wind shear (see Fig. 1(b)). We will consider incorporating these concepts together shortly.

However, before doing so we need to consider what will happen to the eddy over a moderately long period of time. It might be considered that the 'stretching' shown in Fig. 1(b) is only a transient event. After all, the eddy will rotate, and after a quarter cycle it will be aligned against the mean shear. Perhaps then the shear could act to return the eddy to its original isotropic shape (as shown in Fig. 2(a))?

In fact it is unlikely that this will ever happen. As the eddy rotates, it will also become twisted and stretched in a chaotic manner, so the process is not

reversible. Once it has rotated half a cycle, it is conceivable that the mean wind will again try to return the eddy to its original shape, but in fact it will only succeed in twisting and deforming the shape even further, as shown in Fig. 2(b). This process will be especially enhanced by the presence of larger scale eddies in the vicinity which will also impart their own shearing and tearing motions to the eddy. It should also be remembered that the picture often invoked to describe a turbulent 'eddy' – namely a quasi-isotropic ellipsoid – is really only a statistical representation of an 'average' eddy, but in reality true turbulent entities will be highly stretched and distorted 'strings'.

We may now return to our mathematical analysis. The amount of horizontal stretching will be given by $\Delta x \sim (\Delta v)t$, where Δv is the velocity difference between the top and bottom of the eddy, or $\Delta v = (d\bar{u}/dz)l_z$. If we consider the diffusive and wind-shear induced stretching to be additive, then we may write

$$l_x \sim \sqrt{(\beta \epsilon t^3)} + \frac{d\bar{u}}{dz} l_z t. \quad (4)$$

However, we already know that $l_z^2 = \beta \epsilon t^3$ from (3), so we may use this to substitute for t in the above equation. We are especially interested in the degree of isotropy, so let us examine the ratio l_x/l_z . We therefore have

$$\frac{l_x}{l_z} \sim 1 + \left| \frac{d\bar{u}}{dz} \right| l_z^{2/3} \beta^{-1/3} \epsilon^{-1/3}. \quad (5)$$

This is the term which we seek, and it shows clearly that, for larger eddies, the degree of anisotropy is larger – a result which might be expected intuitively, since larger eddies are longer lived and have more time to suffer the effects of wind shear.

As noted earlier, there will be a weak attempt to try to 'recompress' the original eddy after a half and cycle rotation, but this tendency will be small at best, since it will result in a significant decrease in entropy; we will consider that such recompressions do not occur. Thus the second term on the right hand side of the above equation might be reduced by a constant multiplicative factor, but the factor will not be too much different from 1, and we therefore take our expression to still be valid. We write

$$\frac{l_x}{l_z} = \Xi \sim 1 + \gamma \beta^{-1/3} \epsilon^{-1/3} \mathcal{A} \quad (6)$$

where

$$\mathcal{A} = \left| \frac{d\bar{u}}{dz} \right| l_z^{2/3} \beta^{-1/3} \epsilon^{-1/3} \quad (7)$$

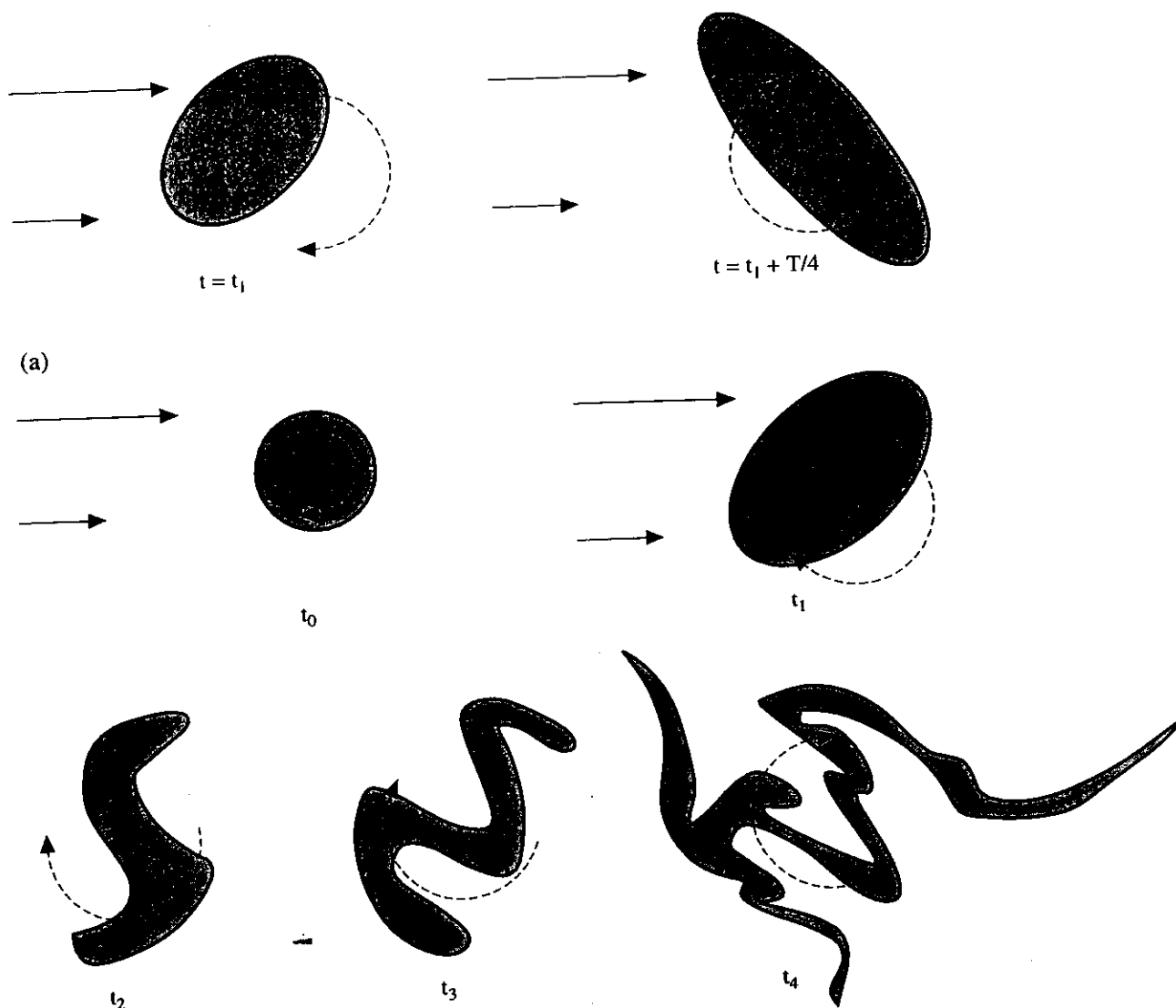


Fig. 2. (a) A schematic of the relation of an eddy in relation to the wind shear after it has rotated one quarter of a cycle. (b) A more realistic representation of the way in which an eddy is distorted by a wind shear as time progresses.

is a dimensionless parameter which we will denote as the 'eddy anisotropy factor' and γ is a constant of order 1, perhaps a bit less than unity. We denote the ratio L_x/L_z by the symbol Ξ .

3. THE RELATION TO ATMOSPHERIC BUOYANCY

At first sight, it appears that the atmospheric buoyancy does not appear in this equation, but in fact this bears further investigation. Let us examine the above ratio for the special case that $l \sim L_B$, where L_B is the buoyancy scale, given by $L_B \approx 10\epsilon^{1/2}\omega_B^{-3/2}$ (Weinstock, 1978). If we substitute $\omega_B = 2\pi/t_B$, then we obtain $t_B \approx 1.3L_B^{2/3}\epsilon^{-1/3}$. We may therefore substitute directly for $L_B^{2/3}\epsilon^{-1/3}$ in our expression (6) to give

$$\frac{L_{Bx}}{L_{Bz}} \sim 1 + 0.75\beta^{-1/3}\gamma \left| \frac{d\bar{u}}{dz} \right| t_B \quad (8)$$

or

$$\frac{L_{Bx}}{L_{Bz}} \sim 1 + 0.75 \times 2\pi\beta^{-1/3}\gamma \left| \frac{d\bar{u}}{dz} \right| \omega_B^{-1}. \quad (9)$$

The term $|d\bar{u}/dz|\omega_B^{-1}$ is just the square root of the inverse of the Richardson number, so we can rewrite this as

$$\frac{L_{Bx}}{L_{Bz}} \sim 1 + \frac{1.5\pi\beta^{-1/3}\gamma}{\sqrt{R_i}} \quad (10)$$

where R_i is the Richardson number. Thus we see that the degree of anisotropy at the larger scales of the turbulent regime are very simply related to the Richardson number. For turbulence generated by a dynamic instability process ($R_i \sim 0.25$), we see that the ratio is approximately between 6 and 10 if we use $\beta = 1$ and take γ to be in the range 0.5–1.0. Note also the weak dependence of the anisotropy on β ; we see that if we use $\beta = 0.5$ (as suggested as an alternative possibility following equation (1)), then the ratio L_{Bx}/L_{Bz} is in the range 7–13 for γ in the range between 0.5 and 1.0 (which is still quite comparable to the range 6–10 which was deduced for the choice of $\beta = 1$). For convectively generated turbulence, the above expression cannot be applied, and we need to revert to the earlier equation (6).

4. APPLICATION IN RADAR STUDIES

One of the chief applications of this work is to studies of aspect-sensitivity in radar studies. However, with a radar one cannot measure the quantity l_z exactly; rather, the radar selectively scatters from eddies with sizes comparable with the radar wavelength. Therefore we need to recast (6) in terms of a radar wavelength, or some related parameter.

We begin by defining a new parameter, \mathcal{A}_π , where

$$\mathcal{A}_\pi = \left| \frac{d\bar{u}}{dz} \right| k_z^{-2/3} \zeta^{-1/3} \quad (11)$$

and where k_z is the vertical wave number ($k_z = 2\pi/\lambda_z$). This clearly is related to \mathcal{A} , but is not exactly the same as it. Note that we should *not* write $k_z = 2\pi/l_z$, since l_z is a measure of the width of an eddy, not a wavelength scale. To see this, consider an eddy with an ellipsoidal shape and with a Gaussian variation in density perturbation, having a half-power half-width ζ . Then the Fourier transform is also a Gaussian with half-power half-width $k_{0.5} \sim (0.22)(2\pi)/\zeta \sim 1.4/\zeta$; this is *not* $k_z = 2\pi/\zeta$.

With this definition of \mathcal{A}_π , equation (6) becomes

$$\frac{l_x}{l_z} \equiv \Xi \sim 1 + \beta^{-1/3} \gamma_\pi \mathcal{A}_\pi \quad (12)$$

where γ_π is another constant.

We can obtain an estimate for the constant γ_π in terms of γ in the following way. We begin by following Hocking (1987) and Briggs and Vincent (1973), where it was shown that the eddy which is most efficient in back-scattering electromagnetic radiation of wavelength λ is one with a $1/e$ half-depth h_e equal to about

0.2λ . Since l_z is the RMS full-depth of an eddy, we may use the fact that $l_z = 2h_e/\sqrt{2}$ to give

$$l_z \approx 0.28\lambda. \quad (13)$$

The Bragg scale λ_c associated with this wavelength is $\lambda_c = \lambda/2$, so that the Bragg wavenumber which is most efficient at producing radar backscatter for this eddy is

$$k_z = 2\pi/\lambda_c = 2\pi(0.28)2/l_z = 3.5/l_z. \quad (14)$$

Substitution into (11) and comparison with (7) then gives $\mathcal{A}_\pi = 0.43 \mathcal{A}$, so that $\gamma_\pi = 2.3\gamma$. If γ is typically within the range 0.5–1.0, then γ_π is in the range 1.15–2.3, and at this stage (and without experimental verification) we suggest that a value of $\gamma_\pi = 2$ is most reasonable. Conversion of l_x/l_z to an effective θ_x (and conversely) can then be accomplished using the expressions discussed by Lesicar and Hocking (1992) and Lesicar *et al.* (1994), viz.

$$\left(\frac{l_x}{l_z} \right)^2 = \left(\frac{\lambda^2/h^2}{8\pi^2 \sin^2 \theta_x} + 1 \right) \quad (15)$$

where λ is the radar wavelength and h is the e^{-1} half-depth of the eddy. The latter has been shown by Hocking (1987) to lie in the range 0.15λ to 0.32λ . Generally a value of $h \approx 0.2\lambda$ is used (also see the discussion prior to equation (13)).

5. INERTIAL SUBRANGE COSPECTRAL PREDICTIONS

The previous development has highlighted the importance of the parameters \mathcal{A} and \mathcal{A}_π in describing the degree of anisotropy of typical eddy structures. It is of significant interest to recognize that this parameter can also occur in other calculations which relate to anisotropy in turbulence. To see this, we consider the velocity cospectrum,

$$E_{uu}(k) = \int_0^\infty \langle u(x)u(x+r) \rangle \cos kr dr. \quad (16)$$

In this case we have simply let k be the wave number along any chosen direction of motion through the turbulence – though of course we must recognize that if the turbulence is anisotropic then the variation in the cospectrum as a function of wave number will differ in scale for different directions of traverse, though it will probably retain the same form. Nevertheless, this is not too important in our following discussion, provided that this fact is recognized.

Our main interest here is in the spectral behavior of the velocity cospectrum in the inertial range where the viscous effects do not play a significant role. Lumley (1967) and Wyngaard and Cote (1972), by assuming

that the cospectrum in the inertial range depends only on k , on the rate of energy dissipation per unit mass ϵ , on the mean shear $|d\bar{u}/dz|$, and assuming further that it is linear in the mean shear, have shown by dimensional arguments that:

$$E_{uu}(k) = - \left| \frac{d\bar{u}}{dz} \right| \epsilon^{1/3} k^{-7/3} \mathcal{F} \left(\left| \frac{d\bar{u}}{dz} \right| \epsilon^{-1/3} k^{-2/3} \right) \quad (17)$$

We see here again the importance of the parameter $\mathcal{A}_\pi = |d\bar{u}/dz| k^{-2/3} \epsilon^{-1/3}$, i.e. equation (17) can be rewritten as

$$E_{uu}(k) = - \epsilon^{2/3} k^{-5/3} \mathcal{A}_\pi \mathcal{F}(\mathcal{A}_\pi). \quad (18)$$

Note that we choose this form for the relation because it still allows us to highlight the classical $\epsilon^{2/3} k^{-5/3}$ dependence on ϵ and k , which is well known for classical Kolmogoroff inertial range turbulence. Because of the importance of \mathcal{A}_π , we will incorporate it wherever possible into the following discussions, although we note that this was not done in some of the references quoted.

At large wave numbers one reproduces Lumley's (1967) result, namely

$$E_{uu}(k) = - \epsilon^{2/3} k^{-5/3} \mathcal{A}_\pi \mathcal{F}(0). \quad (19)$$

In terms of a dimensionless measure of anisotropy, we can divide by $E_{uu} = \alpha_{uu} \epsilon^{2/3} k^{-5/3}$, where $\alpha_{uu} \simeq 0.25$ (as seen in Hocking, 1986, Appendix A); we recognize that E_{uu} here is the same as Θ_{11} there. We then obtain a cospectral anisotropy function $\phi(k)$ where

$$\phi(k) = \frac{E_{uu}(k)}{E_{uu}(k)} = C \mathcal{A}_\pi \quad (20)$$

and where C is a constant. Wyngaard and Cote (1972) went on to generalize the previous result to the case when buoyancy is added to the problem. They showed that the cospectrum is then found to be

$$E_{uu}^B(k) = - \epsilon^{2/3} k^{-5/3} \mathcal{A}_\pi \mathcal{F}(\mathcal{A}_\pi; R_i) \quad (21)$$

which reduces to the previous result in the absence of buoyancy. In the large wave number limit \mathcal{A} tends to zero and they obtained:

$$E_{uu}^B(k) = - \mathcal{F}(0; R_i) \mathcal{A}_\pi \epsilon^{2/3} k^{-5/3} \quad (22)$$

The cospectral anisotropy function can now be written as

$$\phi^B(k) = \mathcal{G}(R_i) \mathcal{A}_\pi. \quad (23)$$

In the case $k = k_n$, the buoyancy wave number, we

may apply similar arguments to those in Section 3 to give

$$\phi^B(k_n) = C_2 \frac{\mathcal{G}(R_i)}{\sqrt{R_i}} \quad (24)$$

where $\mathcal{G}(R_i) = \mathcal{F}(0; R_i)$. Note that this has some features in common with (10), especially the inverse $\sqrt{R_i}$ dependence.

We will not pursue this line of argument here, since the last section has been to some extent a review. Our main purpose has been to show that the parameters \mathcal{A}_π and \mathcal{A} occur repeatedly in studies of turbulence anisotropy, and that these quantities can indeed be considered as fundamental to such work. The derivations discussed earlier in this text in relation to individual eddies (which are quite new), and the formulae discussed in the current section, were derived using independent approaches, and yet the same crucial parameter has arisen in both approaches. This gives extra confidence that these approaches are both valid, and reinforces the importance of this parameter. It also substantiates the derivations of the eddy anisotropy factor shown earlier in this text.

6. APPLICATION TO RADAR STUDIES

We now need to examine the implications of these formulae in radar studies of anisotropy. For VHF scatter from the atmosphere, Bragg scales of 3 m are relevant. In the mesosphere, a large wind shear might be $40 \text{ m s}^{-1} \text{ km}^{-1}$, and a typical turbulence intensity might be 0.01 W kg^{-1} (Hocking, 1990). Then we have from (12) that $l_n/l_z \sim 1.2$, where we have used the values of $\gamma_\pi = 2$ and $\beta = 1$ as recommended earlier in the text. Note that greatest anisotropy occurs when turbulence is weak. In conditions of strong turbulence, the more violent motions tend to allow the maintenance of greater isotropy, overcoming the stratifying effect of the mean vertical shear in the horizontal wind. In the stratosphere we might typically take $\epsilon \sim 10^{-6}$ to $10^{-5} \text{ W kg}^{-1}$ (e.g. Barat, 1982), so that $l_n/l_z \sim 3-5$ for $\gamma_\pi \sim 2$. These would have to be regarded as upper limits, since radars are unlikely to detect weaker turbulence. They correspond to values for the radar aspect factor θ , (Hocking, 1987) of $\sim 5^\circ$ to 10° . Smaller values of θ , associated with true turbulent scatter would only be possible with stronger wind shears.

For a medium frequency (MF) radar operating around 2 MHz (e.g. Lesicar and Hocking, 1992; Lesicar *et al.*, 1994), eddies with dominant Bragg scales of the order of 75 m are the most important for radar scatter. If $\epsilon \sim 0.001$ to 0.1 W kg^{-1} , and the mean wind shear is as above, then l_n/l_z will be of the order of 1.5.

3.5. Such values are in excellent agreement with the types of values reported by Lesicar and Hocking (1992) and Lesicar *et al.* (1994) for scatter in the height range 80–100 km. However, this agreement does not prove that all the scatter from 80–100 km altitude at MF is only caused by anisotropic turbulence; a combination of specular reflectors and isotropic turbulence could result in similar values, as could a scenario involving only specular reflectors which contain substantial undulations. The theory presented so far cannot, in itself, prove the existence of anisotropic turbulence. What it can do is place lower limits on the values of θ_s which can be expected because of anisotropic turbulence; thus we can be quite sure that, if we measure values of θ_s which fall below this limit then we truly have a specularly reflecting process at work. Given the controversy about the nature of these highly specular reflectors/scatters, such a quantitative means of discrimination is important. Let us therefore look at the sorts of lower limits which we might expect in this height range. When $\epsilon \sim 10^{-4} \text{ W kg}^{-1}$ (MF radars are unlikely to detect weaker turbulence), then $I_x/I_z \sim 6$ for $\gamma_\pi \sim 2.0$. Such an aspect ratio would correspond to an aspect sensitivity factor θ_s of $\sim 5^\circ$. Even smaller values would then require massive wind shears, or a completely new explanation such as specular reflections. In fact as a rule we can then say that values of θ_s less than about $4\text{--}5^\circ$ are really caused by specular processes at work. Nevertheless, each case should be treated on its own merits. If it is actually possible to measure the wind shear and the strength of turbulence, even more accurate estimates on the lower limits for θ_s caused by anisotropic turbulence can be made. For the first time, the tools are now available through equations (6) and (12) to assess quantitatively the likely cause of highly aspect sensitive echoes in any given situation.

We conclude this section with a brief discussion about the implications of these results in relation to the ability of radars and *in-situ* probes to measure turbulence, although we emphasize that this is not the main point of this work. To begin, we must note that an upward-pointing radar which utilizes the so-called 'spectral width' method to measure the strength of turbulence (e.g. Hocking, 1985) generally measures the root-mean-square vertical fluctuating velocity within the turbulent patch. It is then assumed that the turbulence is isotropic, and that the level of fluctuation in the horizontal x and y directions is similar. If, however, the turbulence is anisotropic, this can no longer be true.

An exact determination of the correction to the energy dissipation rate must recognize that the anisotropy term is scale dependent, and in addition recog-

nize that the classical $k^{-5/3}$ form of the spectrum will no longer be exactly true, at least for the vertical fluctuating velocities. It is necessary to re-derive the longitudinal spectral function for velocities, and then integrate this spectrum over all wave numbers, after suitably weighting the function by the radar volume. Note that the effective anisotropy term for these calculations is not the anisotropy factor relevant at the scales of the radar wavelength, but an anisotropy factor averaged over all scales from the radar wavelength to the buoyancy scale. An example of this integration for the case of isotropic turbulence has been shown in Hocking (1996), but extension to the anisotropic case is difficult. As it turns out, it is also largely unnecessary for this article, because the anisotropy factor Ξ is only a weak function of ϵ . An error in estimating ϵ by a factor of 3 leads to an error of only 40% in $(\Xi - 1)$. For a typical value of Ξ of say 3, the subsequent error in θ_s is typically about 30%. This is still adequate for us to resolve between anisotropic turbulence and specular reflection in many instances. Thus for the purposes of this article, which is to place limits on the degree of aspect-sensitivity expected for backscatter of electromagnetic radiation by anisotropic turbulence, high precision measurements of ϵ are not required. Further, it is important to recall that our objective here is to place lower limits on the value of θ_s which may be expected because of anisotropic turbulence, so that smaller values can be identified as true specular scatterers. Thus if we err on the small side in our calculations of θ_s , as we will if we under-estimate the strength of turbulence, we can be even more certain that values of θ_s which fall below this limit really are specular reflectors; so in this sense there is little disadvantage in under-estimating ϵ .

For measurements of energy dissipation rates using *in-situ* probes in the presence of anisotropic turbulence the situation is a little easier, provided that the probe can measure to scales within the viscous range. We recognize that the energy dissipation rate is given by

$$\epsilon = 2\nu \int_0^\infty k^2 E(k) dk, \quad (25)$$

where ν is the molecular kinematic viscosity coefficient (e.g. Batchelor, 1953, equation 5.2.9). If it is possible to measure all three components of the wind field, then the above equation can be applied directly, without error. However, even if only one component of the wind is available, it is still possible to make useful estimates by treating the field as isotropic. To see this, we note that the above integral is dominated by scales in the viscous range and at the high wave-number end of the inertial range, where the turbulent eddies are

most nearly isotropic, even in the presence of a wind shear (as clearly seen in our earlier work). Thus direct application of the above equation, but deriving $E(k)$ under the assumption of isotropy, will not lead to huge errors in ϵ in this case.

Further discussion of the topic of how these corrections for anisotropy in estimating ϵ should be made is beyond the objectives of this paper. Certainly future work on anisotropy should involve more detailed determinations of how one might use the radar spectral widths to accommodate any anisotropy in the turbulence field, and it may be possible to draw on the fact that a radar can measure θ_s to help out in this regard. However, we should not lose sight of the original objective of this paper, which was certainly not to develop such a generalized, all-encompassing theory. Rather, it was simply to try to place lower limits on the expected values of θ_s which can be associated with anisotropic turbulence, and thereby help distinguish between specular reflection and anisotropic turbulence. The fact that the anisotropy term involves $\epsilon^{-1/3}$ means that the dependence on ϵ is weak. This enables us to make meaningful estimates of these limits, and such limits have been presented; an error in estimates of ϵ of even a factor of 2 or 3 still makes for reasonable estimates of anisotropy. We are, for example, in a position now to be quite sure that the highly aspect-sensitive reflectors reported by Hocking *et al.* (1991), which had values of θ_s of less than 1° , were not caused by turbulence. Other similar reports of high levels of anisotropy can similarly be ascribed to specular reflectors. In general, a value of θ_s of less than about 4° or 5° can generally be taken to indicate a specularly reflecting process.

We should also finally note that these tests for specularity are essentially one-sided. They can be used to determine if a reflector is truly specular by determining if the measured value for θ_s falls well below the minimum value expected for anisotropic turbulence, but the converse need not apply -- a large value of θ_s (say 8° or 10°) does not necessarily imply that the radar returns must have been caused by turbulent scatter. A specular reflector with substantial wobbles in the reflecting surface could produce quite large values of effective θ_s , certainly up to 10° , as may a combination of specular reflectors and isotropic turbulence.

7. CONCLUSIONS

New expressions have been developed for a quantitative measure of the degree of anisotropy in atmospheric turbulence. This anisotropy factor is a function of the eddy scale, the wind shear, and the strength of turbulence. There is also a Richardson number dependence at the buoyancy scale.

We find that, in the stratosphere for VHF radar studies, the ratio of the length to the depth of a 'typical' eddy should always be less than about 5, so that the aspect sensitivity factor θ_s should be greater than 5° in all cases of turbulent scatter. The only exceptions might be in conditions of unusually strong wind shears. Smaller values, like those reported by Hocking *et al.* (1991), are indicative of a reflection mechanism other than turbulence, and scatterers which induce such narrow backscatter angles can truly be called 'specular'. For MF studies in the mesosphere, I_x/I_z should typically be around 1–4, consistent with observations above 80 km altitude, but in extreme cases could be as high as 6 or so. In such cases, θ_s could be as low as 5° . Lesser values of θ_s would have to be caused by some specular reflection process.

We emphasize that the value of the current work is in its ability to determine how small θ_s must be in order for an observer to be certain that experimental observations represent specular reflection; observed values less than this limit can be ascribed to specular processes. In contrast, it should be noted that, if an observed value for θ_s exceeds the lower limit calculated using this theory, it does not mean that the backscattering medium must have been turbulent; we need to use other sorts of evidence to resolve the cause of the backscatter in this case. This point has been strongly noted in the text. Thus the most important results from this work rest with equations (6) and (12), which may be utilized to allow estimates of the degree of turbulence anisotropy once $|d\bar{n}/dz|$ and ϵ are known, and these estimates can then be used as a benchmark to determine whether specular reflection is the dominant cause of radar scatter in cases of small θ_s .

Acknowledgements Preliminary advice from Dr T. E. Van Zandt after reading an earlier draft is gratefully acknowledged. This work is supported by the Natural Sciences and Engineering Research Council (NSERC) of Canada.

REFERENCES

- Barat J. 1982 Some characteristics of clear air turbulence in the middle stratosphere. *J. atmos. Sci.* **39**, 2553–2564.

- Batchelor G. K. 1950 The application of similarity theory of turbulence to atmospheric diffusion. *Quart. J. Roy. Meteorol. Soc.* **76**, 133-146.
- Batchelor G. K. 1953 *The Theory of Homogeneous Turbulence*, Cambridge University Press, p. 197.
- Bradshaw P. 1975 *An Introduction to Turbulence and its Measurement*, Pergamon, 218 pp.
- Briggs B. H. and Vincent R. A. 1973 Some theoretical considerations on remote probing of weakly scattering irregularities. *Australian J. Phys.* **26**, 805-814.
- De Wolf D. A. 1983 A random-motion model of fluctuations in a nearly transparent medium. *Radio Sci.* **18**, 138-142.
- Doviak R. J. and Zrnic D. S. 1984 Reflection and scatter formula for anisotropically turbulent air. *Radio Sci.* **19**, 325-336.
- Fukao S., Sato T., Kato S., Harper R. M., Woodman R. F. and Gordon W. E. 1979 Mesospheric winds and waves over Jicamarca on May 23-24, 1974. *J. geophys. Res.* **84**, 4379-4386.
- Gage K. S. and Green J. L. 1978 Evidence for specular reflection from monostatic VHF radar observations of the stratosphere. *Radio Sci.* **13**, 991-1001.
- Hocking W. K. 1979 Angular and temporal characteristics of partial reflections from the D-region of the ionosphere. *J. geophys. Res.* **64**, 845-851.
- Hocking W. K. 1985 Measurement of turbulent energy dissipation rates in the middle atmosphere by radar techniques: a review. *Radio Sci.* **20**, 1403-1422.
- Hocking W. K. 1987 Radar studies of small scale structure in the upper middle atmosphere and lower ionosphere. *Adv. Space Res.* **7**(10), 327-338.
- Hocking W. K. 1989 *Target Parameter Estimation, Middle Atmosphere Program Handbook*, Vol. 30, SCOSTEP Secretariat, University of Illinois, pp. 228-268.
- Hocking W. K. 1990 Turbulence in the region 80-120 km. *Adv. Space Res.* **10**(12), 153-161. [*Cospar International Reference Atmosphere*, 1986, Part II, Middle Atmosphere Models, (Rees D., Barnett J. J. and Labitzke K., eds)].
- Hocking W. K. 1996 An assessment of the capabilities and limitations of radars in measurements of upper atmosphere turbulence. *Adv. Space Res.* **17**(1), 37-47.
- Hocking W. K., Fukao S., Tsuda T., Yamamoto M., Sato T. and Kato S. 1990 Aspect sensitivity of stratospheric VHF radiowave scatterers, particularly above 15 km altitude. *Radio Sci.* **25**, 613-627.
- Hocking W. K., Fukao S., Yamamoto M., Tsuda T. and Kato S. 1991 Viscosity waves and thermal-conduction waves as a cause of 'specular' reflectors in radar studies of the atmosphere. *Radio Sci.* **26**, 1281-1303.
- Hocking W. K. and Röttger J. 1983 Pulse-length dependence of radar signal strengths for Fresnel backscatter. *Radio Sci.* **18**, 1312-1324.
- Lesicar D. and Hocking W. K. 1992 Studies of seasonal behaviour of the shape of mesospheric scatterers using a 1.98 MHz radar. *J. atmos. terr. Phys.* **54**, 295-309.
- Lesicar D., Hocking W. K. and Vincent R. A. 1994 Comparative studies of scatterers observed by MF radars in the southern hemisphere mesosphere. *J. atmos. terr. Phys.* **56**, 581-591.
- Lindner B. C. 1975a The nature of D-region scattering of vertical incidence radio waves. I: Generalized statistical theory of diversity effects between spaced receiving antennas. *Australian J. Phys.* **28**, 163-170.
- Lindner B. C. 1975b The nature of D-region scattering of vertical incidence radio waves. II: Experimental observations using spaced antenna reception. *Australian J. Phys.* **28**, 171-184.
- Lumley J. L. 1967 Similarity and the turbulent energy spectrum. *Phys. of Fluids* **10**, 855-858.
- Reid I. M. 1990 Radar observations of stratified layers in the mesosphere and lower thermosphere (50-110 km). *Adv. Space Res.* **10**(10), 107-119.

- 1020
- W. K. Hocking and A. M. Hamza
- Röttger J. and Liu C. H. 1978 Partial reflection and scattering of VHF radar signals from the clear atmosphere. *Geophys. Res. Lett.* **5**, 357-360.
- Röttger J. and Vincent R. A. 1978 VHF radar studies of tropospheric velocities and irregularities using spaced antenna techniques. *Geophys. Res. Lett.* **5**, 917-920.
- Tsuda T., Sato T., Hirose K., Fukao S. and Kato S. 1986 MU radar observations of the aspect sensitivity of back-scattered VHF echo power in the troposphere and lower stratosphere. *Radio Sci.* **21**, 971-980.
- Vincent R. A. 1973 The interpretation of some observations of radio waves scattered from the lower ionosphere. *Australian J. Phys.* **26**, 815-827.
- Vincent R. A. and Belrose J. S. 1978 The angular distribution of radio waves partially reflected from the lower ionosphere. *J. atmos. terr. Phys.* **40**, 35-47.
- Waterman A. T., Hu T. Z., Czechowsky P. and Röttger J. 1985 Measurement of anisotropic permittivity structure of upper troposphere with clear-air radar. *Radio Sci.* **20**, 1580-1592.
- Weinstock J. 1978 On the theory of turbulence in the buoyancy subrange of stably stratified flows. *J. Atmos. Sci.* **35**, 634-649.
- Woodman R. F. and Chu Y. -H. 1989 Aspect sensitivity measurements of VHF backscatter made with the Chung-Li radar: plausible mechanisms. *Radio Sci.* **24**, 113-125.
- Wyngaard J. C. and Cote O. R. 1972 Cospectral similarity in the atmospheric layer. *Quart. J. R. Met. Soc.* **98**, 590-603.

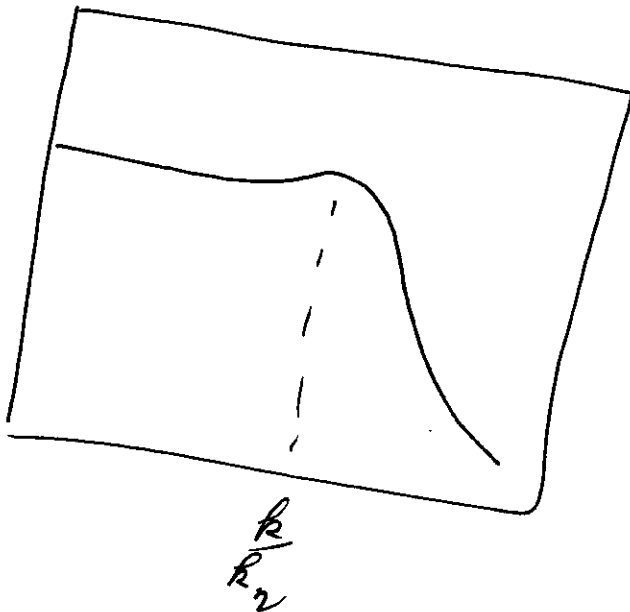


In the last year or so, an exciting new technique has been developed to measure the strength of turbulence. It is described in the following pages.

(Van Zandt et al.)

It is based on theoretical developments due to R. Hill

$$\frac{\phi(k)}{k^{-5/3}}$$



A dual-wavelength radar technique for measuring the turbulent energy dissipation rate ϵ

T. E. VanZandt, W. L. Clark, K. S. Gage,
C. R. Williams¹, and W. L. Ecklund¹
NOAA Aeronomy Laboratory, Boulder, Colorado

Abstract. We used the ratio of simultaneous observations of radar reflectivity by S- and UHF-band radars together with Hill's model of refractivity fluctuations due to turbulence to infer ϵ , the rate of viscous dissipation of turbulent kinetic energy per unit mass. Observations were made for 25 days from November 13 to December 7, 1995, at 11.4°S, 130.4°E (about 100 km northwest of Darwin, Australia) during the Maritime Continent Thunderstorm Experiment (MCTEX). The 500 m pulse length data covered the height range 872 to 3032 m MSL. The observed distribution of ϵ has a strong diurnal variation, with mean daytime and nighttime values of ϵ of the order of 10^{-3} and 10^{-5} m²s⁻³, respectively. With the dual-wavelength technique most non-turbulent echoes (including particulate echoes) are identified and filtered out, since the ensemble of turbulent observations is identified by its conformity to Hill's model. The technique is self-calibrating, requiring only the relative calibration of the two radars using observations during rain, and does not require precise absolute calibration of either radar.

Introduction

The rate of dissipation of turbulence kinetic-energy density ϵ [m²s⁻³] is a basic parameter of turbulence, since it determines the amplitude of the turbulent energy spectrum in the inertial range and the large-wavenumber cutoff of that range. Several techniques have been developed to measure ϵ , but the in situ techniques — aircraft and balloon — are limited in their temporal and spatial extent, lidar techniques are still under development and in any case will not be able to observe through clouds, and the conventional radar techniques require significant corrections due to instrumental and atmospheric effects [Gossard *et al.*, 1998].

The present observations were made from November 13 to December 7, 1995, during the Maritime Continent

Thunderstorm Experiment (MCTEX) with colocated S- and UHF-band wind profiling radars at 11.4°S, 130.4°E, 7 m MSL, in the Tiwi Islands about 100 km northwest of Darwin, Australia [Ecklund *et al.*, 1999; Gage *et al.*, 1999]. The parameters of the S- and UHF-band radars were: frequency, 2835 and 920 MHz; wavelength, 0.1058 and 0.328 m; and beamwidth (FWHP), 3.2° and 9°, respectively. For both radars the beams were directed toward the zenith, the range gates were 500 m, matched in altitude to within a few meters, and the dwell time was 35 s. Only observations matched in time to within ± 35 s were used. The typical interval between observation pairs was a little over six times the dwell time. Observations were analyzed over the altitude range 872 to 3032 m MSL.

Theory of the Dual-Wavelength Technique

The radar reflectivity η_λ [m²/m³] for a given radar wavelength λ [m] can be written [Gossard *et al.*, 1998],

$$\begin{aligned}\eta_\lambda &= \eta_{\text{turb},\lambda} + \eta_{\text{part},\lambda} \\ &= 0.38\lambda^{-1/3}C_n^2 H_{n,\lambda}(\epsilon) + 2.85 \times 10^{-16}\lambda^{-4}Z_e,\end{aligned}\quad (1)$$

where $\eta_{\text{turb},\lambda}$ and $\eta_{\text{part},\lambda}$ are the contributions due to scattering from turbulent irregularities of the refractive index n and to scattering from particulates, respectively. C_n^2 [m^{-2/3}], the turbulence structure constant of n , and Z_e [mm⁶m⁻³], the rain-equivalent reflectivity factor, are independent of λ and depend only on the properties of the turbulence field and of the ensemble of particulate scatterers, respectively.

The λ^{-4} dependence in $\eta_{\text{part},\lambda}$ holds for particulate scatter in the Rayleigh range; that is, from particulates with an effective diameter $\leq \lambda/10$ [Battan, 1973]. For the S- and UHF-band wavelengths used in this study, all particulates except large hail, birds, airplanes, etc. lie in the Rayleigh range.

The $\lambda^{-1/3}$ dependence in $\eta_{\text{turb},\lambda}$ holds for Bragg scatter from turbulent fluctuations of the radio refractive index n in the inertial-convective range. The factor $H_{n,\lambda}(\epsilon)$ takes into account departures from the $\lambda^{-1/3}$ behavior when viscosity and diffusion are important. Hereafter $H_{n,\lambda}(\epsilon)$ will be approximated by the [Hill, 1978] model factor for turbulent fluctuations of temperature $H_{T,\lambda}(\epsilon)$ (henceforth simplified to $H_\lambda(\epsilon)$), which

¹Also with the Cooperative Institute for Research in the Environmental Sciences (CIRES), University of Colorado, Boulder, Colorado

is an excellent approximation to $H_{n,\lambda}(\epsilon)$ as long as the temperature-humidity cospectrum is positive. The argument of $H_\lambda(\epsilon)$ is usually expressed as $\kappa\eta_0$, where $\kappa = (4\pi/\lambda)$ is the Bragg wavenumber for radar backscatter, $\eta_0 = (\nu^3/\epsilon)^{1/4}$ is the Kolmogorov microscale, and ν is the kinematic viscosity, a known function of atmospheric temperature and density. Thus, at a given altitude $\kappa\eta_0$ is a function of ϵ parametric in λ .

Curves of $\log[H_\lambda(\epsilon)]$ (where $\log \equiv \log_{10}$) for an altitude of 1592 m MSL and the present radars are plotted (thin curves) in Figure 1(a) versus $\log[\epsilon]$ for ϵ from 10^{-6} to 10^{-2} [m^2s^{-3}]. When ϵ is sufficiently large, a radar signal is scattered from turbulent irregularities in the inertial-convective range and $H_\lambda(\epsilon) = 1$. As ϵ decreases, $H_\lambda(\epsilon)$ increases to a small peak (≈ 1.5) in the viscous-convective range and then decreases rapidly to very small values in the viscous-diffusive range.

The value of ϵ can be inferred only when $\eta_{turb,\lambda}$ is dominant in both η_S and η_U , so that it is convenient to transform η_λ to

$$C_\lambda \equiv \frac{\eta_\lambda}{0.38\lambda^{-1/3}} \quad (2)$$

$$= C_n^2[H_\lambda(\epsilon) + B\lambda^{-11/3}Z_e/C_n^2],$$

where $B = 7.50 \times 10^{-16}$, and to form the ratio

$$\frac{C_S}{C_U} = \frac{H_S(\epsilon) + B\lambda_S^{-11/3}Z_e/C_n^2}{H_U(\epsilon) + B\lambda_U^{-11/3}Z_e/C_n^2} \quad (3)$$

Then, when η_{turb} predominates in both C_S and C_U ,

$$C_S/C_U \approx [H_S(\epsilon)/H_U(\epsilon)], \quad (4)$$

which connects the observations with turbulence theory. The heavy curve in Figure 1(a) is the ratio $H_S(\epsilon)/H_U(\epsilon)$

plotted as a function of ϵ . Since $H_U \approx 1$ over the range of interest, then $C_U \approx C_n^2$ according to Equation 2.

Conversely, when $\eta_{part,\lambda}$ predominates in both C_S and C_U , then

$$\log[C_S/C_U] \approx \log[(\lambda_S/\lambda_U)^{-11/3} = 62] = 1.79. \quad (5)$$

Results

As an example of the application of this technique, we show the analysis and results of the MCTEX observations at 1592 m MSL, although the data from all heights have been analyzed. First, the color 2D-histogram in Figure 1(b) shows the percentage of the 13,478 observations of $\log[C_S/C_U]$ occurring within each pixel of $\log[C_S/C_U]$ versus $\log[C_U]$ at this altitude. The sensitivity limit of the UHF-band radar bounds the left side of the plot. Only those occurrences for which the S- and UHF-band vertical velocities differed by $\leq 1 \text{ ms}^{-1}$ have been accepted. This almost entirely eliminates spurious side-lobe echoes from strong non-atmospheric targets such as birds, bats, or airplanes.

The power of these dual-wavelength systems to delineate the nature of atmospheric scatterers [Gage et al., 1999] is apparent in Figure 1(b). The upper occurrence-density ridge is produced by Rayleigh, or particulate, scatter (the downward curvature on the right is due to saturation of the S-band receiver). The relative calibration of the radars is established by slightly adjusting the $\log[C_S/C_U]$ ratios so that this ridge is centered on the theoretical value of $\log[C_S/C_U] = 1.79$ for Rayleigh scatter (see Equation 5), represented by the upper dashed line. The abscissa has been truncated to emphasize the turbulent scatter region, but Rayleigh scatter was actually observed out to $\log[C_U] \approx -8.7$, corresponding to $Z_e \approx 45 \text{ dB}$.

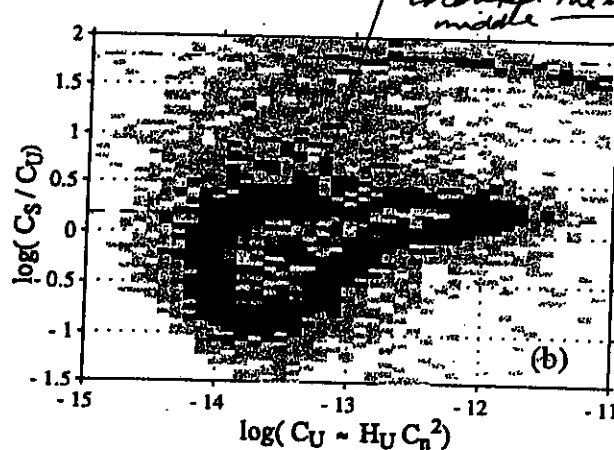
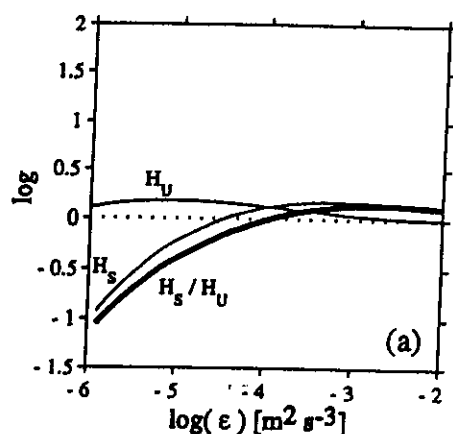


Figure 1. (a) The thin curves labeled H_U and H_S represent the log of Hill's [1978] model factors to correct the inertial-convective range spectrum for the effects of viscosity and diffusion. The heavy curve labeled H_S/H_U depicts the log of this ratio, which models C_S/C_U versus ϵ for pure turbulent scatter. (b) A 2D histogram of the percentage occurrence in each 0.1 by 0.1 pixel of $\log[C_S/C_U]$ versus $\log[C_U]$ of the 13,478 total observations taken during MCTEX at 1592 m MSL. The middle dashed line indicates the peak model value of $\log[H_S/H_U]$. The upper dashed line indicates the theoretical value for pure Rayleigh scatter.

The similarity between the shape of the lower ridge in Figure 1(b) and the model curve of $\log[H_S(\epsilon)/H_U(\epsilon)]$ in Figure 1(a) strongly indicates this ridge is due to turbulent scatter. Indeed, since the abscissas in Figures 1(a) and (b) have been scaled so that three decades of $\log[\epsilon]$ have the same length as two decades of $\log[C_U] \approx \log[C_n^2]$, much of the ridge is consistent with $\epsilon \propto (C_n^2)^{3/2}$, as suggested by heuristic theory [Gage et al., 1980; Hocking and Mu, 1997]. The occurrences between the upper and lower ridges are due to mixed particulate and turbulent scatter.

The relation between $\log[C_S/C_U]$ and ϵ is only weakly dependent on local environmental conditions [Hill, 1978]. Thus, a particular value of $\log[C_S/C_U]$ in the turbulent ridge can be identified with the same value of $\log[H_S(\epsilon)/H_U(\epsilon)]$, which then determines the corresponding value of ϵ . Figure 2 shows the distribution of occurrences of $\log[\epsilon]$ versus local solar time (LT = UCT + 0841 h). During MCTEX, sunrise and sunset were at 0530 h and 1810 h LT, respectively, plus or minus a few minutes. Between 08 and 09 h (about 3 h after sunrise) the mean ϵ increases abruptly from its nighttime value of about $10^{-5.2}$ to a mean of about $10^{-3.5}$ [m^2s^{-3}] through midday and then decreases back to the nighttime value by 23 h. The peak value generally occurs near midday between 1500–1600 m MSL. The shape of the diurnal variation in Figure 2 is consistent with the strongly convective daytime atmosphere at this location [Ecklund et al., 1999; Gage et al., 1999]. As the altitude increases from 872 to 3032 m, the diurnal variation changes in three ways: a) the morning increase starts later; b) the afternoon decrease starts earlier; c) the nighttime values increase slightly, probably due to the decrease of radar sensitivity.

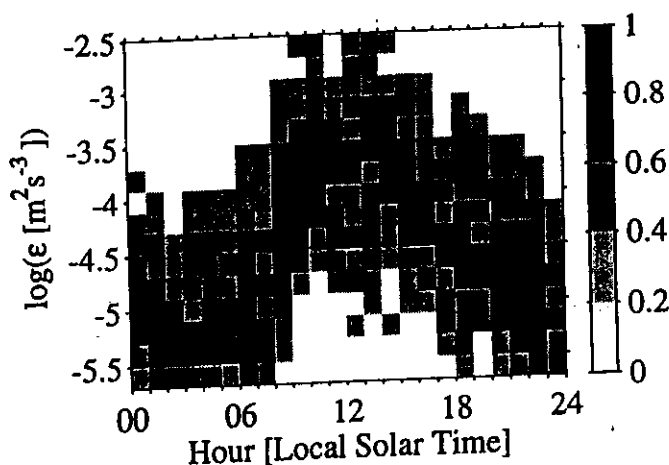


Figure 2. A set of vertical histograms showing the number of occurrences of particular values of $\log[\epsilon]$ at 1592 m MSL. A histogram is plotted for every hour of local solar time (LT), normalized by the peak number of occurrences for that hour. The 8694 values of ϵ are from the lower ridge of $\log[C_S/C_U]$ values in Figure 1(b).

The measured daytime values of ϵ are fairly consistent with those in other studies (e. g., see the review by [Hocking and Mu, 1997]). Of course, as ϵ approaches 10^{-3} , the curve of H_S/H_U becomes flat so that the inferred values of ϵ become sensitive to small errors in either C_S/C_U or the model. Indeed, not using occurrences of $\log[C_S/C_U] > 0.18$ (the maximum value of $\log[H_S/H_U]$), which are probably valid observations but with small positive errors), reduces the histogram of ϵ there. However, the absence of occurrences with $\log[C_U] > -11.5$ in Figure 1(b) is consistent with a lack of values of ϵ larger than about $10^{-2.5}$.

If larger values of ϵ were anticipated at other locations, the range of ϵ could be extended by using a shorter wavelength radar (e. g., 3 cm), though the increased sensitivity to Rayleigh scatter from insect and cloud particles might result in an increased fraction of particulate echoes.

The nighttime values of order 10^{-5} presented here are uncertain because the observations of C_S and C_U were near instrumental limits. Although not inconsistent with the typical values found in other studies of background turbulence (see Table 4, [Gultepe and Starr, 1995]), values approaching 10^{-7} have also been observed. Of course, the dual-wavelength observations could be extended to smaller ϵ by using more sensitive or longer wavelength radars.

Although not a factor in this study, H_S/H_U is sensitive to the specific humidity q when the Tq cospectrum is strongly negative [Hill, 1978]. Then the peak value of H_S/H_U is increased slightly and the curve is shifted toward smaller ϵ . However, even in the "extreme" case in Figure 3 of [Hill, 1978], the present estimates of $\log[\epsilon]$ would be only about 0.3–0.4 too small, except near the peak of H_S/H_U . Inspection of simultaneous balloon profiles of T and q from 26 km southwest of the radars shows that large negative Tq cospectra are rare during this campaign.

A further complication to these studies can arise if there is a negative correlation between ϵ and C_n^2 within the pulse volume, such as is thought to exist in shear-generated turbulence [Gibson-Wilde et al., 1999], which would lead to systematically small values of ϵ . The present daytime observations were taken during convection when such a negative correlation would not obtain, but such an effect on the nighttime values cannot be ruled out.

Examination of Figure 1(b) shows that, for any given value of observed $\log[C_U]$, a spread of $\log[C_S/C_U]$, or values of ϵ , is observed. This may be attributed in large part to the dependence on q and dq/dz of the relation between ϵ and C_n^2 (e. g., Hocking [1997]). This interpretation is supported by the fact that the spread is much smaller in similar dual-wavelength observations (not shown) taken at the Flatland Atmospheric Observatory in Illinois in winter where q and dq/dz are small.

The theory assumes, of course, that the mean value of ϵ is the same in the observation volumes of the S- and

UHF-band radars. But because the beamwidths of the radars were different (3.2° and 9° , respectively), spatial variations across the beams will lead to fluctuations of $\log[C_S/C_U]$, that spread the turbulent ridge but do not bias the mean values of C_S/C_U and ϵ . Because the 9° beam is only about 250 m in diameter at 1592 m, the spatial variations here should be small.

This technique could be used to measure ϵ in other environmental regions, such as the stratosphere or the ocean (using sonars), as long as $k\eta_0 = (4\pi\nu^{3/4})/(\lambda\epsilon^{1/4})$, the argument of Hill's factor, for the shorter-wavelength sounder lies between about 0.3 and 1.0. Further work is needed to extend the technique to both higher and lower values of ϵ , to measure ϵ under other meteorological conditions, and to make simultaneous measurements with other techniques.

Acknowledgments. We thank Rod Frehlich (CIRES, University of Colorado), Earl Gossard (CIRES and NOAA Environmental Technology Laboratory (ETL)) and Reginald Hill (NOAA ETL) for comments and clarifications on the material presented here. We thank Paul Johnston (CIRES and NOAA Aeronomy Laboratory) for his significant role in implementation and operation of the radar systems. This research was supported in part by the National Science Foundation under Grants ATM-9214800, the NOAA Office of Global Programs, and DOE ARM.

References

- Battan, L. J., *Radar Observation of the Atmosphere*, 324 pp., Univ. Chicago Press, Chicago, revised ed., 1973.
- Ecklund, W. L., C. R. Williams, and P. E. Johnston, A 3-GHz profiler for precipitating cloud studies, *J. Atmos. Ocean. Technol.*, **16**, 309–322, 1999.
- Gage, K. S., J. L. Green, and T. E. VanZandt, Use of Doppler radar for the measurement of atmospheric turbulence parameters from the intensity of clear-air echoes, *Radio Sci.*, **15**, 407–416, 1980.
- Gage, K. S., C. R. Williams, W. L. Ecklund, and P. E. Johnston, Use of two profilers during MCTEX for unambiguous identification of Bragg scattering and Rayleigh scattering, *J. Atmos. Sci.*, **56**, 3679–3691, 1999.
- Gibson-Wilde, D., J. Werne, D. Fritts, and R. Hill, Direct numerical simulation of VHF radar measurements of turbulence in the mesosphere, *Radio Sci.*, **35**, 783–798, 1999.
- Gultepe, I. and D. O'C. Starr, Dynamical structure and turbulence in cirrus clouds: Aircraft observations during FIRE, *J. Atmos. Sci.*, **52**, 4159–4182, 1995.
- Gossard, E. E., D. E. Wolfe, K. P. Moran, R. A. Paulus, K. D. Anderson, L. T. Rogers, Measurement of clear-air gradients and turbulence properties with radar wind profilers, *J. Atmos. Ocean. Technol.*, **15**, 32–342, 1998.
- Hill, R. J., Spectra of fluctuations in refractivity, temperature, humidity, and the temperature-humidity cospectrum in the inertial and dissipation ranges, *Radio Sci.*, **13**, 953–961, 1978.
- Hocking, W. K., and P. K. L. Mu, Upper and middle tropospheric kinetic energy dissipation rates from measurements of C_n^2 — review of theories, in situ investigations, and experimental studies using the Buckland Park atmospheric radar in Australia, *J. Atmos. Solar-Terr. Phys.*, **59**, 1779–1803, 1997.
- W. L. Clark, W. L. Ecklund, K. S. Gage, T. E. VanZandt, C. R. Williams, NOAA Aeronomy Laboratory R/AL3, 325 Broadway, Boulder, CO 80305. (e-mail: wclark@al.noaa.gov, wle@al.noaa.gov, kgage@al.noaa.gov, vanzandt@al.noaa.gov, chris@al.noaa.gov)

(Received March 22, 2000; revised June 16, 2000; accepted June 19, 2000.)

6.6.3.5 Determinations of K

Measurements of K (either K_m or K_T) are also important in atmospheric studies. However, techniques vary widely, and are not always consistent. We have seen relations like $K = c\varepsilon/(\omega_B^2)$, and such relations may well apply within a particular layer of turbulence. On the other hand, when we examine diffusion over spatial scales of tens of kilometres vertically, it is not clear what the appropriate diffusion coefficient might be, particularly in view of the fact that layers of turbulence can often be separated by regions of laminar flow. How does one determine an effective diffusion coefficient in this case? Dewan (1981; *Science*) and Rastogi and Woodman have pointed to a process involving stochastic and intermittent creation and destruction of turbulent layers, so that the rates of diffusion depend not only on the strengths of turbulence but also on the rates of creation, and the lifetimes, of these turbulent layers.

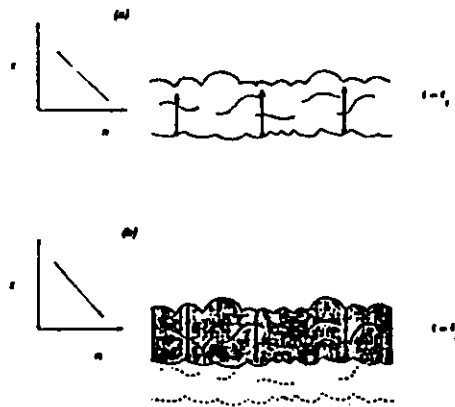


Fig 27. Illustration of the process of atmospheric vertical diffusion proposed by DEWAN (1981) and WOODMAN and RASTOGI, (1984). (a) A layer of turbulence forms at time t_1 and constituents diffuse against their background gradient. The small graph on the left-hand side shows a representative profile of the mean density of a constituent, and in this case diffusion will be upwards across the layer. (b) Constituents could only diffuse across the layer in (a), and no further, because the layer has a limited depth. The layer in time dies out, and this decayed layer is shown as the broken line. Eventually, at some later time t_2 , a new layer forms above the present one, and is then able to allow further diffusion of the constituents upward. The overall rate of large scale diffusion therefore depends at least as much on the frequency of formation of these layers as it does on the actual turbulent intensity within the layers.

Additionally, Walterscheid and Hocking (1991) have demonstrated the possible importance of "Stokes diffusion" as a possible mechanism for diffusion of constituents in the atmosphere. All these processes need to be recognized, and it may be that the most appropriate diffusion process may be a function of scale.

Therefore, in the following section I am going to list several different procedures which have been used in the past to measure diffusion coefficients. Some can be performed with radar, some cannot. I will not be "judging" the optimum technique: I will simply be noting them.

Clearly the first technique, then, is to use measurements of ε and the Brunt-Vaisala frequency to determine K through the relation

$$K = c\varepsilon/(\omega_B^2) \quad (127)$$

An example of an extensive set of measurements by this method is that presented by Fukao et al., (1994).

One of the main applications of diffusion coefficients is for numerical modeling of large scale atmospheric motions. Thus another common means by which diffusion coefficients are inferred is to use numerical models "in reverse", leaving the diffusion coefficients as free parameters and "tuning" the K values so the results of the model agree best with experimental observations.

Whilst a few attempts have been made to determine K from direct experimental observations, they have not been frequent. Justus, (1967a) tried to obtain K_m and K_t separately from detailed measurements of wind velocity, and from observing the oscillation amplitude of eddies. Another attempt to determine K directly was tried by Zimmerman and Keneshea, (1981) who used rocket measurements of temperature to solve the equation

$$K_t = -\overline{w'\Theta'} / (d\overline{\Theta}/dz) \quad (128)$$

Θ being potential temperature and w' the vertical fluctuating velocity. Additionally, Vincent and Stubbs, (1977) have looked at gravity wave decay with height, although this method has large inaccuracies due to uncertainties in determining "typical" vertical wavelengths for gravity waves. Teitelbaum and Blamont, (1977) also made rocket estimates of K , and Gibbins, et al., (1982) used studies of the transport of water vapour to give estimates of K .

More recently, Weinstock, (1982) has proposed a formula which relates the vertical diffusion coefficient to the mean square fluctuating velocities of gravity waves. This formula has arisen from his work on non-linearity in saturating gravity waves, and takes the form

$$K_m = \sum_m \frac{\overline{w^2(m)}}{2Hk\omega_B} \quad (129)$$

where $\overline{w^2(m)}$ is the mean square fluctuating vertical velocity of gravity waves with vertical wavenumber m , H is the scale height, and ω_B is the Brunt-Vaisala frequency. The parameter k is a "typical" horizontal wavenumber for waves of vertical wavenumber m . Preliminary estimates of K using variations of this formula have been made by Vincent, (1984) and Meek et al., (1985). It should be noted that the formula does require the existence of a saturated gravity wave spectrum. Measurements of K by this type of procedure almost certainly refer to large scale diffusion processes. The gravity wave approach for estimation of K has been compared to the eddy diffusion approach in a review by Ebel, (1984).

As already noted, direct measurements do not represent the major means by which K has been determined. More commonly, estimates of K have been made by comparing modeling studies with observed temperature, wind and constituent distributions, and "tuning" the value of K to give best agreement. For example, one of the earliest examples of this type of approach was that due to Johnson and Wilkins, (1965). These authors noted that the temperature gradient at 85-110 km is not as steep as it should be if only molecular diffusion acted, and so Johnson and Wilkins, (1965) concluded that turbulence must be acting to transfer the heat down from the regions where photodissociation (and therefore heating) takes place to the lower regions where CO_2 radiation can occur. Working from this premise they were then able to obtain approximate estimates of the expected eddy diffusion coefficient. In a somewhat similar vein, Colegrove et al., (1965) noted that observed ratios of the concentration of O_2 to that of O at 120 km were higher than might be expected. They postulated that eddy diffusion could mix the O down from 120 km to 90 km, where the mean free path is less, and so allow greater O_2 concentrations in the 90-120 km region. These authors also made estimates

198

of K . These last two techniques form the basis of many subsequent estimates of K . Successive authors have included temporal variations (Shimazaki, 1971; Keneshea and Zimmerman, 1970), and have looked at latitudinal and seasonal variations (Hesstvedt, 1968; Johnson and Gottlieb, 1970; Blum and Schuchardt, 1978). It was also pointed out (Keneshea and Zimmerman, 1970) that some of the earlier papers had assumed that turbulence existed above the turbopause and therefore were in error. Strobel et al., (1987, 1989) and Garcia and Solomon, (1985) have used even more sophisticated models to estimate K_m and K_T . These latter models treated K_T and K_m as separate parameters, and inferred that K_m is somewhat larger than K_T by a factor of about 3 times (Strobel, 1989).

An interesting question arises from this work on energy and oxygen balance. Turbulence produces both heating and diffusion, and it is not at all obvious which process dominates. The rate of diffusion of heat depends on both the turbulent diffusion coefficient K and the vertical temperature gradient, the latter being caused initially by solar heating. Both Johnson and Gottlieb, (1970) and Johnson, (1975) pointed out that the rates of diffusion and heating are very similar. The question arises as to which is most effective - is diffusion more effective, so that turbulence actually diffuses heat across the heat gradients formed by solar effects faster than it causes heating itself (and thus cooling the mesosphere), or is it more efficient at depositing heat, thus heating the mesosphere? It turns out that the answer to this question lies in the value of the constant c_2 in equation (24), but no definitive reference exists which can unambiguously say which process dominates.

The reason for the dependence on c_2 can be seen by examining the Richardson number R_i . This is given by

$$R_i = \frac{\omega_B^2}{(d\bar{u}/dz)^2} = \frac{\omega_B^2}{\epsilon/K_m}, \quad (130)$$

since $\epsilon = K_m(d\bar{u}/dz)^2$ (Justus, 1967a). Here $d\bar{u}/dz$ is the vertical shear in the mean wind. Thus $K_m = c_2\epsilon/\omega_B^2$, where $c_2 = R_i$ is the mean Richardson number of all turbulent patches. Hunten, (1974) showed that the rate of transfer of heat through the mesosphere was $F = nH\rho\omega_B^2 K$, (where $n = 7/5$, H = scale height, ρ = density), whilst the rate of loss of heat over one scale height was $P = (R_i)^{-1} H\rho\omega_B^2 K$. Thus $P/F = (R_i n)^{-1}$.

Clearly heating dominates if $\bar{R}_i \leq 0.28$, and diffusion if $\bar{R}_i \geq 0.28$. Hunten, (1974) claimed that for turbulence to occur, R_i must be less than 0.25 so heating should dominate, whilst Johnson, (1975) claimed that whilst R_i must be less than 0.25 to initiate turbulence, turbulence may then persist for values of R_i as high as 1.0. Thus Johnson, (1975) claimed that \bar{R}_i is nearer 1.0. The estimates suggested earlier (equation (24)) would imply that diffusion dominates. Recently Chandra, (1980) has presented a more rigorous treatment of estimation of eddy diffusivities to bring into account c_2 and assumed $c_2 = 0.6$, and Gordiets et al., (1982) have concluded that the answer to the question of whether turbulence heats or cools its immediate environment depends on the height gradient of K . They claimed that turbulence heats below about 105 km altitude and cools above.

One problem with these theoretical estimates of K is that they do not consider the effects of vertical winds. For example, atomic oxygen from 120 km could be brought down to 90 km by vertical winds at one location, and lifted back up by vertical winds at another. The possibility of such "cells" of circulation has not been included in any of these analyses. Thus, in principle, all prior estimates are upper limits of K .

The following paper
summarizes ~~the~~ the main
concept which we have established
in the last few pages.

The dynamical parameters of turbulence theory as they apply to middle atmosphere studies

W. K. Hocking

The University of Western Ontario, London, Ont., Canada

(Received August 21, 1998; Revised January 20, 1999; Accepted April 12, 1999)

The study of turbulent heating and diffusion in the middle atmosphere is complicated by some subtle points relating to the application of existing theory. Incorrect interpretation of turbulent spectra can result, leading to errors in estimates of the strengths of turbulence by factors of 5 and more. In this short review, the relevant turbulent spectra and equations are considered, and their applications in middle atmosphere studies are outlined. New developments with regard to some of this theory, and especially new understandings about the dynamical parameters used in some of these applications (often referred to as the “constants” of the equations) are described. Current areas of uncertainty are also considered, both in relation to turbulent energy dissipation as well as diffusion over various scales.

1. Introduction

In studies of turbulence, the optimum spectra to use for calculations of kinetic energy dissipation rates are often the velocity spectra. These are dealt with in some detail in the literature (e.g. Batchelor, 1953; Tatarskii, 1961, 1971). For freely decaying turbulence we can consider ε , the kinetic energy dissipation rate, as

$$\varepsilon = -\frac{d}{dt} \frac{1}{2} [\overline{u^2 + v^2 + w^2}], \quad (1)$$

where $\overline{u^2 + v^2 + w^2}$ is the total mean square velocity fluctuation, and $\frac{1}{2} [\overline{u^2 + v^2 + w^2}]$ is therefore the mean kinetic energy per unit mass at any instant in time (Batchelor, 1953, page 86). The overbar refers to a spatial average. (An even more fundamental discussion about the energy dissipation rate can be found in Batchelor, 1967, Subsection 3.4, but that is beyond our requirements for this paper.)

If an experimentalist can obtain velocity fluctuations at scales within the inertial range of turbulence, or even into the viscous range, then calculation of kinetic energy dissipation rates is very straight forward. For example, if an observer is dealing with isotropic, homogeneous turbulence, and if that observer can make measurements at scales within the inertial range and deep into the viscous range, then the kinetic energy dissipation rate ε can be found directly by integrating across the spectrum as

$$\varepsilon = 2 \int_0^\infty \nu k^2 E(k) dk \quad (2)$$

where ν is the kinematic molecular viscosity coefficient, k is the wave number, and $E(k)$ is the spectral density of velocity fluctuations (sum of all three components) over a shell

in wave-number space of radius k (e.g. see Batchelor, 1953; Hocking and Hamza, 1997, and references therein). However, in atmospheric sciences, determination of $E(k)$ down to scales this small is rarely possible. In the middle atmosphere, it simply cannot be achieved with current technology.

If it is possible to determine velocity fluctuations down to scales at least into the inertial range, determination of ε is still modestly easy, although one often needs to make assumptions about the form of turbulence (isotropic, Kolmogoroff theory etc.). Examples of such applications exist in the literature: for example, Barat (1982) has shown how this may be done using structure functions.

However, Barat's measurements required a high altitude balloon, and special instrumentation. Measurements into the upper middle atmosphere by this method are limited by a ceiling on the balloon altitude. In-situ measurements above say 40 km altitude are limited to rockets, and because these must travel at high speed, they cannot sample the velocities with sufficient resolution to apply such methods.

Measurements of middle atmosphere turbulence are therefore largely limited to radar techniques, and occasional rocket and balloon studies. Within these categories, only special balloon-borne instrumentation is capable of direct velocity measurements at sufficient spatial and temporal resolution to enable direct calculation of ε , and even then high altitude balloons are only flown rarely. All other methods involve measurements of velocity fluctuations which effectively integrate over moderately large intervals of scale, or involve measurements of parameters other than the velocity fluctuations. In the former case, the integration limits and instrumental weighting are often hard to determine, and in the latter case it is often necessary to make various assumptions, and determine other parameters such as background gradients, before turbulence strengths can be calculated.

This review focuses on a critical examination of the assumptions made in developing the formulae which are used in determination of middle atmosphere turbulence strengths,

and highlights recent developments in this area.

2. Currently Used Formulae

The following equations present various formulae which are currently used for determinations of middle atmosphere turbulence strengths.

$$\varepsilon = c_0(\sigma^2)^{3/2}/L_B, \quad (3)$$

$$L_B = \frac{2\pi}{c_3} \varepsilon^{1/2} \omega_B^{-3/2}, \quad (4)$$

$$\varepsilon = c_1(\sigma^2)\omega_B. \quad (5)$$

Variations of these formulae have been presented by, for example, Weinstock, (1978a,b, 1981), and Hocking (1983, 1986). The term ω_B is the Väisälä-Brunt frequency, ε is the kinetic energy dissipation rate, σ refers to a typical root-mean-square velocity (to be specified in more detail later), and L_B is a scale related to the larger eddies.

These equations appear deceptively simple, but they are in fact complicated by several factors. Principal amongst these is the fact that the term σ^2 is sometimes ill-defined. The constants c_0 and c_1 are critically dependent on how σ^2 is determined. Formulae of this type are often used in both in-situ and radar studies, but the nature of the determination of σ^2 must be very carefully considered. For example, in radar studies it is usually an integral over the radar volume, and over the duration of the radar record used for the calculation. The details of this integration process need to be carefully considered. As we will see, there are also additional complications, and even the choice of the scale L_B is complicated.

In fact there are some references which use yet another variant on Eq. (3). This equation takes the form

$$\varepsilon = c_6(\sigma^2)^{3/2}/L_r \quad (6)$$

where L_r is a scale associated with the radar beam and pulse-length, and not the scale L_B defined above (e.g. Labitt, 1979; Bohne, 1982; Doviak and Zrnic, 1984). We therefore need to ask: which of these two options (i.e. Eqs. (3) or (6)) is preferable?

Thus we recognize that these equations, despite a deceptively simple appearance, are not well understood, and we pose the questions: What do we mean by σ^2 ? Which scale " L " should we use? Answering these questions will be one of our responsibilities in this paper.

There are also other equations which appear in the literature which need to be more properly understood. Some such equations are the expressions

$$\eta = \left(\frac{\nu^3}{\varepsilon}\right)^{1/4}, \quad (7)$$

$$\ell_0 = c_4 \eta \quad (8)$$

and

$$L_B = c_5 L_0. \quad (9)$$

Again, these are very simple equations, but with hidden complications. We will define the various terms and consider these expressions shortly.

Another expression used in the literature to determine ε , which utilizes the mean square refractive index fluctuation quantity C_n^2 , is

$$\bar{\varepsilon} = \left(\gamma \overline{C_n^2} \frac{\omega_B^2}{F^{1/3}} M^{-2}\right)^{3/2}. \quad (10)$$

C_n^2 is often called the "potential refractive index structure constant", although the use of the word "constant" here can be quite misleading, since the quantity is far from constant—it in fact varies markedly as a function of the intensity of the turbulence. Nevertheless, we must persist with this usage, since it is very common. However, the reader should bear in mind that C_n^2 is in fact a measure of the amount of refractive index fluctuation in a given turbulent patch, and is not to be considered in the same category as the other dynamical parameters (also referred to as "constants") which are the topic of this paper. Again, the above expression looks simple enough, but application of this expression is complicated by determination of the term " F " (which represents the fraction of the radar volume which is turbulent), and by a proper determination of the "constant" γ —which in fact turns out to be Richardson-number dependent. We will not consider the factor " F " any further here; our main interest is in the parameter γ . Discussions relating to " F " can be found in Van Zandt *et al.* (1978, 1981) and Hocking and Mu (1997).

Finally, there is another expression which appears to be exquisitely simple, yet hides a multitude of complexity. This is the expression

$$K = c_2 \frac{\varepsilon}{\omega_B^2} \quad (11)$$

where K represents a diffusion coefficient. This relation purports to relate the rates of atmospheric diffusion and the value of the kinetic energy dissipation rate. However, it raises many issues. It may be derived from modestly simple arguments; for example, Fukao *et al.* (1994), Appendix A, gives one example. However, there are yet further questions about this. Is the derivation too simplistic? Is it valid at all? If it is valid, what should be the "constant" c_2 ? Different authors have proposed different values for c_2 . If indeed it does apply, is it valid over all scales? If the scale-range is limited, what limits exist? McIntyre (1989) has even considered that the value of c_2 might depend in some way on the mode of turbulence generation, and the degree of super-saturation of the waves which generate the turbulence. How realistic is this proposal? In that case, it would not even make sense to assume that c_2 is a constant for an individual event, although there might still be some long-term average value of c_2 which can be applied to the middle atmosphere. We cannot address all these issues, but will try and consider at least some of them.

Thus, while we recognize that these formulae are used in the literature for determination of ε and K , we also recognize that each equation embodies a complication of one sort or another. A major objective of this paper will be to highlight, and where possible clarify, these complications.

We will begin our discussions by pointing the reader to Appendices A to D, which contain expressions for the currently accepted structure functions and spectra which are generally used in theoretical Kolmogoroff turbulence studies. In general the formulae are presented without proof: they are meant

202
to simply be a summary of the main and simplest tools used in turbulence studies. We begin with functions associated with measurements of velocity, and later move to measurements of tracers and scalars.

In our next sections, we then begin to address some of the questions raised above.

3. Turbulence Scales and Inverse Scales

We first turn to a discussion of the Eqs. (7) to (9), mainly because the questions posed in relation to these expressions are some of the simplest to answer.

The first equation, (7), is a derivation produced from dimensional analysis. However, once derived it can be usefully employed as a scaling length. Physically, it is a scale within the viscous range of the turbulence, and represents a typical scale at which energy transfer by scale-cascade, and energy dissipation to heat, are comparable. The scale ℓ_0 is a scale which represents the transition between the inertial and viscous ranges of turbulence, and is defined in terms of the intercept between extrapolations of the spectral forms in these two ranges (e.g. see Tatarskii, 1971). It is always bigger than η , and the constant c_4 is in fact fairly well known. However, it is important to recognize that even c_4 depends on whether one is using measurements of velocity fluctuations or some sort of constituent or tracer. Typical values of c_4 are 7.4 for temperature fluctuations (e.g. Hill and Clifford, 1978), and $(15C)^{3/4}$ (where $C = 2.0$), or 12.8, for velocity fluctuations (e.g. Tatarskii, 1961).

Thus these scales are at least fairly well understood, although on occasions some authors have assigned them to have units of *metres per radian*, which is wrong. They are simply units of length.

Equation (9) does introduce some extra complications, however, which sometimes lead to confusion. The scale L_0 is a vertical scale at which the RMS fluctuations due to the turbulence are equal to the change in the mean value of the same quantity over the same vertical scale. This is quite different to L_B , which is a scale at the "large-scale end" of the inertial range of the spectrum. The latter quantity is usually much larger than the first—often by more than an order of magnitude (e.g. see Hocking, 1985, who gives a ratio in the order of 30).

To complicate things further, an alternative scale to L_B is often used, which equals $\varepsilon^{1/2} \omega_B^{-3/2}$ and is called the Ozmidov scale. This differs from L_B only by a multiplicative constant of $2\pi/c_3$, so conceptually is very similar to L_B . We will generally use L_B , since this has become more common in middle atmosphere work, and Barat (1982) has shown that it does indeed seem to relate fairly nicely to the low wavenumber end of the inertial range.

Another common problem which occurs in discussions about the scales of turbulence is the use of inverse scaling factors. Whilst a scale is assigned a "wavelength" λ , and its corresponding wavenumber is $k = 2\pi/\lambda$, it is not uncommon to use special inverse scales which relate to particular spatial lengths by a simple reciprocal relation. For example, sometimes a scale $k_B^* = 1/L_B$ is used for scaling purposes. This seems at odds with the wavenumber $k_B = 2\pi/L_B$, but in fact there is no conflict; we will therefore dispense with this issue here. L_B is a "typical" scale, but does not particularly

represent the distance between the maxima of any special sinusoidal fluctuation. Therefore there is no obligation to use 2π as the scaling constant, so $k_B^* = 1/L_B$ is just as useful for scaling purposes as $2\pi/L_B$. Problems arise, however, when k_B^* is referred to as a "wavenumber"; it is in fact not one, and should be considered (when used) as nothing more than an inverse scaling factor. Confusion arises because scaling parameters like this are sometimes referred to as "wavenumbers", and because they are often denoted by symbols which are traditionally used for harmonic quantities. If, on the other hand, one is talking of true wavenumbers, and their relation to "wavelengths", then one must use $k = 2\pi/\lambda$.

4. Relation between ε and σ^2

In this section, we wish to address the issue of the correct relation between σ^2 and ε , as described in Eqs. (3) and (6). The equations look similar, but in fact are very different conceptually, and we need to understand why.

In studies of turbulence with a radar, one usually measures a complex-amplitude time-series which is a result of radio-wave scatter from a region of space called the "radar volume". This volume is defined by the radar beam and radar pulse-length. Within this volume, scatterers are moving with a variety of velocities, and the observed signal is due to a combination of Doppler shifted echoes produced when the radiowaves scatter from these entities. The received signal can be Fourier transformed to produce a spectrum, which has a half-power half-width of $f_{1/2}$, and an associated variance f_v^2 . If we multiply f_v^2 by $(\lambda/2)^2$, where λ is the radar wavelength, then we produce a variance in terms of velocity units, which we denote as σ^2 . This variance is an integrated effect of all the velocity fluctuations within the radar volume, as shown diagrammatically by Hocking (1983).

Detailed derivations of the relation between the turbulence velocity spectrum (which describes the fluctuations inside the radar volume) and the value of σ^2 have been presented by (amongst others) Hocking (1983), Labitt (1979), Bohne (1982) and Hocking (1996a). In the following subsections, we will briefly re-visit some of these derivations.

To begin, we will follow the derivation presented by Hocking (1983), which produces Eq. (3).

4.1 Buoyancy scale dependence between σ^2 and ε

Assuming a Kolmogoroff form for the turbulence spectrum, Hocking (1983, 1986) has shown that

$$\sigma^2 \propto \int_{2\pi/L_B}^{k=4\pi/\lambda} \varepsilon^{2/3} k^{-5/3} dk, \quad (12)$$

where σ is the root mean square velocity deduced from the spectral width of the signal. At this stage we will not concern ourselves with the constants of proportionality; our main interest here is in the general form of the equation. We will shortly produce a more sophisticated form of this equation in which the relevant constants of proportionality will become clearer. This equation expresses the fact that the velocity variance measured by the radar is the integrated effect of different scales within the radar volume.

Upon integration we obtain the following expression:

$$\sigma^2 \propto \varepsilon^{2/3} \left[L_B^{2/3} - \left[\frac{\lambda}{2} \right]^{2/3} \right]. \quad (13)$$

Assuming that $L_B \gg \lambda/2$ we have the following relationship:

$$\varepsilon = c_1 \frac{\sigma^3}{L_B} \quad (14)$$

The value of c_1 differs somewhat for different assumptions about the constants involved in the Kolmogoroff spectrum, but Hocking (1983) has given a value of c_1 of 3.5. This value assumes that the fluctuations producing the radar signal are produced in roughly equal proportion by scales in the buoyancy range and the inertial range. We shall re-address this assumption shortly.

If, in addition, we use the relation between the buoyancy scale L_B and the Väisälä-Brunt frequency which was specified earlier as

$$L_B = \frac{2\pi}{0.62} \varepsilon^{1/2} \omega_B^{-3/2} \quad (15)$$

(Weinstock, 1978b), we may then write

$$\varepsilon = c_0 \sigma^2 \omega_B \quad (16)$$

where c_0 is a constant (~ 0.45).

In contrast to this expression, (which is commonly used in mesospheric and stratospheric radar studies), equations relating radar spectral widths and turbulent energy dissipation rates which have been presented in the meteorological literature have tended to ignore the possibility that the buoyancy scale may play a role in the relation between ε and σ^2 . Rather, they have assumed that either the length of the radar pulse, or the radar beam-width, (whichever is larger) is the most important parameter in determining this ε — σ^2 relation. We will now look at this particular derivation in more detail.

4.2 Radar volume dependence between σ^2 and ε

The following derivation briefly summarizes that presented by Labitt (1979), and also presented by Hocking (1996a). We do not intend to repeat their derivations in detail here, and so we start with the relation

$$\sigma^2 = \int_{-\infty}^{\infty} \int_{-\infty}^{\infty} \int_{-\infty}^{\infty} \Phi_{ii}(k) [1 - e^{-(k_x^2 b^2 + k_y^2 a^2 + k_z^2 a^2)}] dk, \quad (17)$$

which is derived in those references. Φ_{ij} is described in Eq. (B.4), and in this case we take $i = j$ i.e. both velocity components aligned in the direction parallel to the direction of traverse (in this case the direction of traverse of the radar beam) through the patch of turbulence (see Appendices A to D). The term in square brackets is simply 1 minus the Fourier transform of the radar volume, and therefore takes into account the radar weighting. Equation (17) is in fact similar in some aspects to Eq. (12), but there are also some important differences between the two. The former one essentially assumes that all radial motions are parallel to the bore-sight direction of the radar, while this newer one recognizes that there may be contributions from off-bore-sight components if the beam is broad. Equation (12) also contains no specific radar weighting, but does contain a lower limit on k which is defined by the largest turbulence scales. Equation (17) contains no such turbulence-defined limit, and this will shortly prove to be an important point.

It is also important to point out that neither of these formulae recognize the fact that the velocity spectrum should actually be anisotropic at scales comparable to and larger

than L_B . However, since for MST work the radars usually point vertically, and it is primarily the vertical velocity spectrum which affects the spectral width, it is only necessary that a reasonable estimate of the vertical velocity spectrum is produced for our work here. In this case, we specify $E(k)$, and the vertical velocity spectrum is derived from that, but we have allowed a reasonable range of possibilities for $E(k)$, and therefore a reasonable range of vertical velocity spectra. The key point is that $E(k)$ is chosen so that the vertical velocity spectra are realistic. Since horizontal fluctuations are of secondary significance for a vertically pointed, narrow beam, the issue of anisotropy is not so crucial here. Hocking (1996a), and Hocking and Hamza (1997) has discussed the issues of anisotropy in a little more detail.

If one then takes the classical inertial range spectrum (e.g. see Tatarskii, 1971), then the spectrum of vertical velocities as a function of wave number k is

$$\Phi_{ii}(k) = \frac{E(k)}{4\pi k^2} \left[1 - \frac{k_z^2}{k^2} \right], \quad (18)$$

where k is the magnitude of k and so is a scalar satisfying $k^2 = k_x^2 + k_y^2 + k_z^2$, $E(k) = \alpha \varepsilon^{2/3} k^{-5/3}$, and α is a numerical constant with value 0.7655C, where $C = 2.0$ (see Eq. (B.4)).

The following expression for the velocity variance measured by the radar may now be obtained:

$$\sigma^2 = \frac{1}{2} \alpha \varepsilon^{2/3} \Upsilon, \quad (19)$$

where

$$\Upsilon = \int_{\theta=0}^{\pi} \int_{k=0}^{\infty} \sin^3 \theta k^{-5/3} \times [1 - e^{-k^2 [a^2 \sin^2 \theta + b^2 \cos^2 \theta]}] dk d\theta. \quad (20)$$

Thence

$$\varepsilon = \frac{2\sqrt{2}}{[\alpha \Upsilon]^{3/2}} \sigma^3. \quad (21)$$

Finally, the following expressions for Υ are valid: Firstly if $a \geq b$:

$$\Upsilon = 2\Gamma\left(\frac{2}{3}\right) a^{2/3} F\left[\frac{-1}{3}; \frac{1}{2}; \frac{5}{2}; 1 - \frac{b^2}{a^2}\right] \quad (22)$$

whilst if $b \geq a$:

$$\Upsilon = 2\Gamma\left(\frac{2}{3}\right) a^{2/3} F\left[\frac{-1}{3}; 2; \frac{5}{2}; 1 - \frac{a^2}{b^2}\right]. \quad (23)$$

Where F is the confluent hypergeometric function. To a good approximation we can write

$$\varepsilon = 0.79 \frac{\sigma^3}{L_r} c_c \quad (24)$$

where L_r is the largest of the pulse length and the beam width, and c_c is a correction factor very close to 1.

As noted, Eqs. (14) and (24) are conceptually very different. Why should this be?

The answer to this question can be seen in the diagrammatic sketch shown in Fig. 1. This diagram shows a schematic representation of the spectrum, as well as the weighting effect of the radar beam. It also emphasizes the fact that

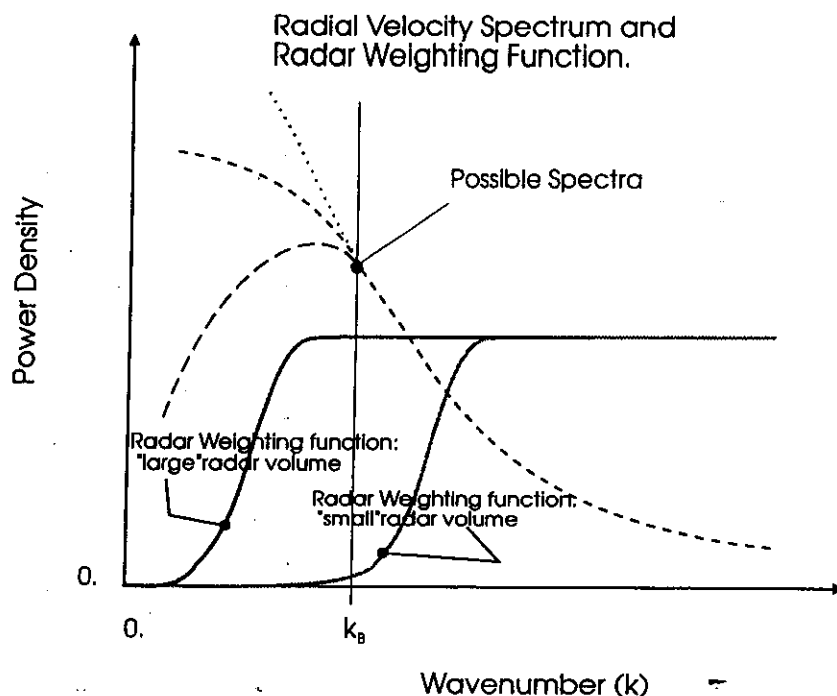


Fig. 1. Graphs showing the radial velocity spectra and radar weighting functions for different assumed spectra and radar volumes.

the spectrum may have a "roll-over" at small wavenumbers, where a "roll-over" refers to a moderately abrupt but smooth change in slope. This may be evident as a "knee" in the spectrum, or even a local peak. Whether such a "rollover" exists depends on what one assumes about the nature of the low wave number spectrum (often the gravity wave spectrum) at the scales close to the turbulence regime. It also depends on which radial velocities are being measured—a vertically pointed radar measures principally the vertical fluctuating motions, whilst a horizontally pointed radar measures largely horizontal components of motion. In our discussion we are primarily considering near-vertical beams, which are the main modes used for middle atmosphere studies.

This "roll-over" is what causes the Labitt formalism to break down. Labitt assumed that the Kolmogoroff spectral form (i.e. $\propto k^{-5/3}$) continued down to $k = 0$, and this is why his integral involves L_r . Such an assumption may be valid if the radar is used to point its beam horizontally (as is the case, for example, with the meteorological NEXRAD radars). However, if this "roll-over point" in the spectrum occurs at wave-numbers which are greater than the lowest wave-numbers corresponding to the radar volume, then the integral begins to involve L_B . For most middle atmosphere radars, near-vertical beams are used, so this latter possibility is likely.

Figure 1 shows how this comes about. The integrand involves a product of the spectrum and the weighting function, and it is seen that if the weighting function is that for a "small" radar volume, and we follow it from large k back to small k , then the weighting drops to zero before k_B is encountered. Thus the integral does not involve any portion of the spectrum at k values below k_B . However, in the case labelled "large

radar volume", the radar weighting function does not start to approach zero (reading from the right) until the spectrum has entered the "buoyancy" regime. Thus the nature of the spectrum in this low wave-number end begins to affect the integral.

The situation is also indicated diagrammatically, but in a different way, in Fig. 2. In the first case, we show a region of turbulence with the radar volume being substantially smaller than the largest scales of turbulence. In this case, we expect the Labitt formula to apply. However, the other diagrams (b, c, and d) show cases where some part of the radar volume exceeds (or is at least comparable with) the largest scales of the turbulence. In this case, we expect the formula with an L_B dependence to apply.

Thus Labitt has ignored the small wavenumber departure from the inertial range law. However, we should also point out that Eq. (12) is also only a crude approximation, since it assumes that the spectrum drops abruptly to zero at the wavenumber k_B . Therefore both approaches have their weaknesses—Eq. (12) is mathematically crude, while Eq. (17) is mathematically rigorous but ignores the true small-wavenumber spectral variation. It makes sense to combine the formalisms, to try and take advantage of both of their strengths.

In the following section, we will put the concepts discussed above into a mathematical setting, and demonstrate that our expectations are valid. In fact, we will show that the largest cross-volume length of the radar volume must be less than one half of the buoyancy scale for the Labitt formula to apply—in all other cases, the formula involving L_B is more appropriate.

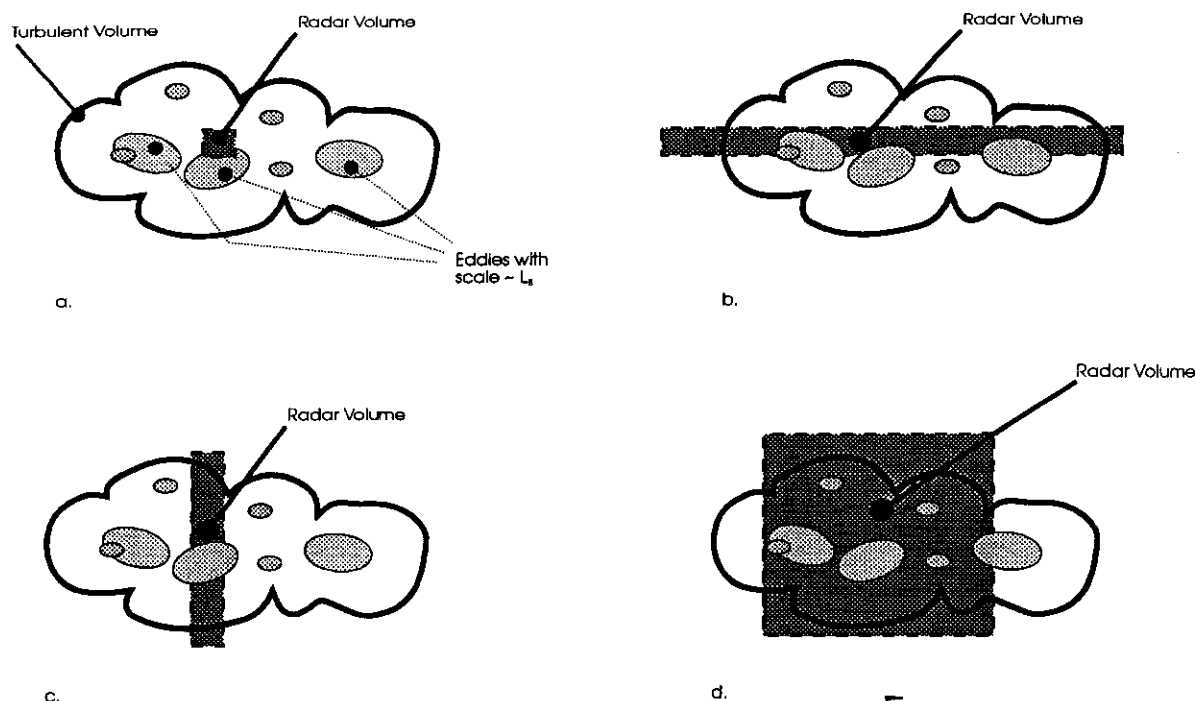


Fig. 2. Different possible relations between the radar volume and a patch of turbulence. Only in the first case is the behaviour of the turbulence spectrum at small k (i.e. below k_B) unimportant in determining the relation between ϵ and σ . In all other cases, the relation between ϵ and σ has a k_B dependence.

5. Combining the Buoyancy Part of the Spectrum within the Labitt-Formalism

We will now re-address Eqs. (17) and (18), but this time we will permit $E(k)$ to have a "roll-over" point at low wave-number. We will see that this substantially changes Eq. (24), and in fact makes the result appear more like (14) in many cases.

To begin, we propose the following possible shape of the spectrum at small k , (as discussed by Hocking, 1996a):

$$E(k) = \alpha \epsilon^{2/3} \frac{k^{-5/3}}{[1 + \chi_k (k/k_B)^n]} \quad (25)$$

where $k_B = 2\pi/L_B$ and where the value of n determines the form of the low wave-number part of the spectrum. The value of χ_k affects the relative positions of the low-wavenumber "roll-over point" in the spectrum and the quantity k_B . Hocking (1996a), used the special cases $n = -3$ and $-4/3$, because they represent extreme examples of the possible spectral forms, and thus set reasonable limits on our formulae. They correspond to cases with $E(k) \propto k^{4/3}$ and $k^{-1/3}$ at small k respectively. Examples are shown diagrammatically in Fig. 3 for the case of $\chi_k = 1.0$. Clearly the "knee" (or "peak" for the case $n = -3$) is close to the value of k_B , so henceforth we will use $\chi_k = 1.0$ as a reasonable approximation, although we recognize that future more detailed experimental studies might give slightly different values for this parameter. At present, however, there are insufficient experimental data to better define χ_k .

As noted prior to Eq. (18), this equation implicitly assumes an isotropic spectrum. However, this is not entirely unreasonable for the cases we wish to consider. In addition, for a vertically directed beam it is principally the vertical velocity

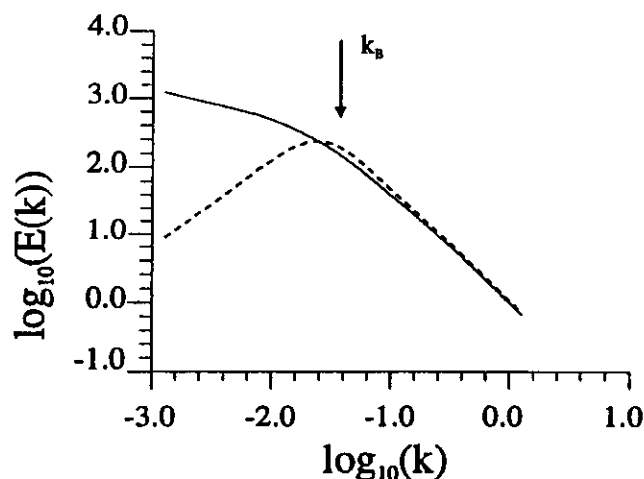


Fig. 3. Representative forms for the turbulence spectrum $E(k)$, including typical possible variations at small k . Specifically these graphs show Eq. (25), for $n = -3$ and $-4/3$. The $n = -3$ case corresponds to a power law of the type $k^{4/3}$ at small k , and is represented by the broken line; the $n = -4/3$ case corresponds to a power law of the type $k^{-1/3}$ at small k , and is represented by the solid line. In both cases the buoyancy scale is the same and equals 250 m; the corresponding wavenumber lies very close to the peak in the broken curve (from Hocking, 1996a).

fluctuations which are important, so as long as $E(k)$ is chosen so as to produce a reasonable vertical velocity spectrum, any lack of isotropy is not too critical to our arguments. It should also be recognized that we only seek to place reasonable limits on the relation between spectral widths and the energy dissipation rates, so great accuracy in specifying $E(k)$ is not required—indeed, it is presently not available



We now must determine

$$\Upsilon = \int_{\theta=0}^{\pi} \int_{k=0}^{\infty} \sin^3 \theta \frac{k^{-5/3}}{[1 + (k/k_B)^n]} \times [1 - e^{-k^2[a^2 \sin^2 \theta + b^2 \cos^2 \theta]}] dk d\theta. \quad (26)$$

any scale, then to very good accuracy, Υ can be represented closely by the following expression:

$$\Upsilon = (0.45L_B)^{2/3}. \quad (27)$$

Hence, using Eq. (21) we obtain the relation

$$\varepsilon = 3.3 \frac{\sigma^3}{L_B} = 0.47 \sigma^2 \omega_B. \quad (28)$$

This compares very favourably to the estimates made in the earlier literature, in which the equation $\epsilon = 0.45\sigma^2\omega_B^2$ has been given e.g. see Eq. (16). Figure 4(a) shows a contour graph in which a measure of the ratio of the true value of ϵ relative to the above formula is shown for various beam

widths and various buoyancy scales L_B . The area in which the Labitt formula is accurate is also highlighted; note that throughout most of the region described by this graph the dependence of ε on L_B is very important and the Labitt formalism is generally not valid. As experimental support for this prediction, it is noteworthy that Bohne (1981: abstract), who attempted to use the Labitt formalism to produce radar measurements of ε , and then compared them with measurements made in-situ, found that he could only make useful estimates of ε for those cases in which the radar pulse length was less than one half of the buoyancy scale. The reason for the inaccuracy of the radar measurement in these cases of small L_B was almost certainly because Eq. (28) should have been used, rather than the Labitt approach.

Let us now turn to the case of $n = -4/3$. In this case the spectrum goes as $k^{-1/3}$ as k tends to 0. Then in fact numerical integration of Eq. (26) over a wide range of possible buoyancy scales and possible pulse lengths and beam widths gives the following expression:

$$\varepsilon = 3.3 \frac{\sigma^3}{L_B} \frac{1}{c_f} = 0.47 \sigma^2 \omega_B \left[\frac{1}{c_f} \right]^{2/3} \quad (29)$$

where c_f is a correction factor. Even in this case, where the buoyancy range runs somewhat smoothly into the inertial range, but where the energy involved in the buoyancy range is higher than that in the inertial range, it can be seen that the dependence on L_B is still significant and the expression given by Labitt is generally not appropriate.

Figure 4(b) shows the value of the correction factor over a wide range of beam widths and buoyancy scales. Note that the region in which the Labitt formalism is approximately correct is indicated and is clearly only a small portion of the region. For MST radars the Labitt equation is almost never valid and the previous expression (29) is correct. Furthermore, the correction factor is a fairly slowly varying term which varies from as small as 0.9 for very small beam widths and very long buoyancy scales up to a factor of as high as 2 for very broad beam widths (widths of several kilometres). The correction factor is dependent on the characteristics of the particular radar being used, but it is not a strong function of the radar parameters, and a reasonable estimate of it can be made in almost all circumstances.

Thus in summary, we see that the correct equations to use for converting σ^2 from radar measurements (after removal of beam and shear-broadening (e.g. Hocking 1983; Nastrom, 1997)) is in fact Eq. (29) with correction factors as shown in Figs. 4(a) or 4(b) (depending on the nature of the spectrum as it goes from the turbulent regime to the gravity wave regime).

We have thus unified the two sets of possible formulae discussed earlier, and also demonstrated when each applies. This is an important result for future applications of radar measurements in studies of turbulence strengths using radars.

We now move on to discussion of the other methods for measurement of atmospheric turbulence. The previous discussion concentrated on measurements of velocity fluctuations, whereas the next section will look in more detail at scalar parameters.

6. Scalar Spectral Methods for Measuring ε

In this section, we will consider measurements of scalar quantities like potential refractive index, neutral fluctuations, and ion and electron densities, and discuss how they may be used to infer ε . We will concentrate on two main areas—firstly, the ways in which radar can be used to measure refractive index fluctuations, and then the ways in which direct in-situ measurements of spectra can be employed to determine ε .

The first case relates to application of Eq. (10), and we now wish to address the questions we have raised in relation to that equation. To begin, we first recognize that C_n^2 is a measure of refractive index fluctuations, and refractive index fluctuations are related more to *potential energy* perturbations and less to kinetic energy fluctuations. Thus the relationship between C_n^2 and ε depends on the ratios of potential to kinetic energy. Since this ratio is Richardson-number dependent, it might not be surprising to find that γ could depend on the Richardson number. Nevertheless, there have been documents in which it has been assumed that γ is indeed a constant, and for a while this was accepted as standard. In the next section, we will re-examine the rather complex history associated with γ . Again, we remind the reader that the terminology of “constant” for C_n^2 is very misleading, but is maintained here for historical reasons. In the following section, we consider C_n^2 not as a true constant, but simply as a variable which parameterizes the degree of potential refractive index fluctuation in a turbulent patch. Our main point of discussion will be the dynamical parameter γ . We emphasize that the following discussion relates both to radar measurements of turbulence strengths using absolute backscatter techniques, as well as in-situ measurements of ion, electron and neutral density fluctuations.

6.1 The “constant” γ

Despite the above expectation about a Richardson-number dependence of γ , for a while this dependence was all but ignored in the literature, and γ was indeed taken as a constant. Examples include Van Zandt *et al.* (1978, 1981), Gage (1980), as well as Hocking (1985), Thrane *et al.* (1985, 1987), Lübken *et al.* (1987) and Blix *et al.* (1990). Note that in the last four cases, it was not actually C_n^2 , the potential refractive index gradient structure “constant”, which was measured, but rather one of the neutral, ion or electron density structure “constants”. Nevertheless, the same principle applied, and in each case the R_i dependence of γ was not properly considered.

This is not to say that the non-constancy of γ was unknown, but rather it was fully appreciated only in fields other than middle atmospheric ones. Examples of references which demonstrate a Richardson number dependence include Ottersten (1969), Crane (1980), and Gossard *et al.* (1982, 1985, 1987). However, for middle atmosphere applications many of these early references were not utilized. To be fair, however, the R_i dependency was often not recognized because it was impossible to employ it, simply because measurements of R_i with sufficient resolution were not possible. More recent papers like Hocking (1992), Blix (1993) and Hocking and Mu (1997) have given due recognition to the more realistic R_i dependence in middle atmosphere applications, but are again constrained by the inability of cur-

rent techniques to make measurements of R_i with sufficient resolution to be useful. Nevertheless, the recognition of this dependence is important from a conceptual viewpoint, which is why we pursue it here.

We will now recap some of the earlier papers which noted that γ was not in fact a constant. Ottersten (1969) gave

$$\gamma = \frac{1}{a^2} \left(\frac{1 - R_f}{R_i} \right) = \frac{1}{a^2 P_r} \left(\frac{P_r - R_i}{R_i} \right) \quad (30)$$

where a^2 is a constant, R_i is the gradient Richardson number, R_f is the flux Richardson number, and $R_f = P_r^{-1} R_i$, P_r being the turbulent Prandtl number. P_r is defined as K_m/K_T , where K_m and K_T are the turbulent momentum and heat diffusion coefficients respectively.

Gossard *et al.* (1982, 1984) present an expression in which γ effectively obeys

$$\gamma = \frac{1}{B_\theta} \frac{P_r - R_i}{R_i} \quad (31)$$

where $B_\theta = 3.2$.

Hocking (1992) assumed to first order a turbulent Prandtl number of unity and obtained, via energy balance arguments, the following expression for γ ;

$$\gamma = \frac{3}{22} \frac{|1 - R_i|}{|R_i|} \quad (32)$$

The ratios of potential to kinetic energy storage as a function of R_i , as deduced by Hocking (1992), are shown graphically in Fig. 5.

We therefore recognize that even when the R_i dependence of γ is understood, there is not general agreement about the details of the relationship. Different authors have produced different relationships, and we cannot resolve these differences here. Our preference is to use Eq. (32).

If Richardson number measurements are not available, then a value of

$$\gamma = 0.4 \quad (33)$$

is recommended as a reasonable compromise, since it corresponds approximately with a Richardson number of 0.25 according to (32). We therefore see that we are once again

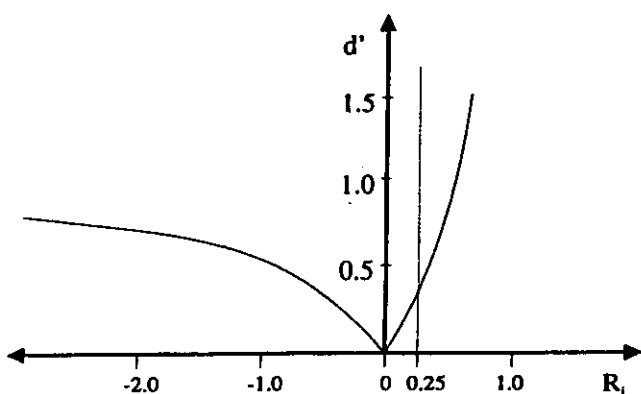


Fig. 5. The ratio of the potential energy and kinetic energy spectral densities, d' , plotted as a function of the Richardson number, R_i . Note that the ratio tends to infinity as R_i approaches 1, and tends to 1 as R_i approaches negative infinity (from Hocking, 1992).

returning to an assumption of a constant value for γ , but this approach is adopted simply because it is often not possible to measure R_i with sufficient resolution. It is fairest to think of this as a mean value for γ . It is often the best we can do, but is definitely an inferior approach to proper use of R_i in determining γ .

6.2 An alternative way to determine ε using spectral fitting around the spectral knee

Because of uncertainties in regard to application of the previously discussed " C_n^2 " method, Lübken *et al.* (1993), and Lübken (1997) developed an alternative method for determination of ε . This method still employs direct measurements of scalar spectra, but in a different manner to that described in the previous section. It has been well-known for many years that if one can measure η , the Kolmogoroff microscale, then one can determine ε through the relation (7). The kinematic viscosity ν is usually taken from empirical atmospheric models. The major difficulty is determination of η accurately, because ε is proportional to η to the fourth power. For example, an error in η of a factor of 2 means an error in ε of a factor of 16. Traditionally η has been determined by finding the inner scale, ℓ_0 , and then determining η through (8) using an assumed value for c_4 . (e.g. Watkins *et al.*, 1988). The value of c_4 depends on whether one is measuring velocity fluctuations, ion fluctuations, neutral fluctuations or whatever, as seen earlier.

This method fell from favour, however, because there was too much uncertainty in determining ℓ_0 . Different extrapolation schemes produced different values. Lübken has recently attempted to solve this difficulty by fitting a carefully prescribed function to the Fourier-spectrum of the time series of neutral density fluctuations measured by a moving rocket (expressed as a function of the spectral angular frequency ω) viz.

$$W(\omega) = \frac{\Gamma(5/3) \sin(\pi/3)}{2\pi v_r} \cdot C_n^2 \cdot f_\alpha \cdot \frac{(\omega/v_r)^{-5/3}}{[1 + \{(\omega/v_r)/k'_0\}^{8/3}]^2} \quad (34)$$

An angular frequency of ω corresponds to a spatial scale in the turbulence along the track of the rocket with "wavelength" equal to $2\pi v_r/\omega$. Here, $\Gamma(5/3) = 0.90167$; v_r is the rocket speed; $f_\alpha = 2.0$, and $k'_0 = 2\pi/\ell'_0$, where ℓ'_0 is a length scale closely related to ℓ_0 . The denominator in the last multiplicative term was introduced as an attempt to allow the inertial range to run smoothly into the viscous range, and is somewhat ad-hoc. Because this is so, it is necessary to exercise some care in the meaning of ℓ'_0 . Lübken *et al.* (1993), and Lübken (1997) made the (unproven) assumption that $\ell'_0 = \ell_0$. We wish to emphasize that because this is not yet proven, it represents a possible source of systematic error in the following discussions, and we will distinguish between ℓ'_0 and ℓ_0 in our discussions here-in, although we recognize that Lübken *et al.* did not. An alternative way to write (34) would be

$$W(\omega) = \frac{\Gamma(5/3) \sin(\pi/3)}{2\pi v_r} \cdot C_n^2 \cdot f_\alpha \cdot \frac{(\omega/v_r)^{-5/3}}{[1 + \chi_r \{(\omega/v_r)/k_0\}^{8/3}]^2} \quad (35)$$

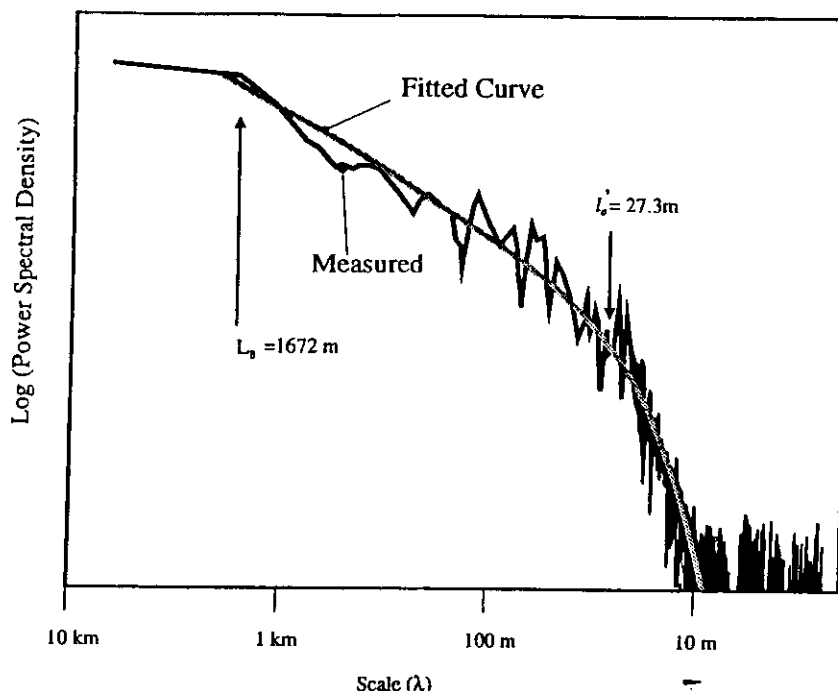


Fig. 6. Experimental and fitted spectra for rocket measurements of neutral density fluctuations. The smooth curve shows a fit assuming a Heisenberg model in the viscous range. Buoyancy and inner scales are also shown (adapted from Lübken, 1997).

where $k_0 = 2\pi/\ell_0$, and the term χ_L accounts for the fact that the spectral “knee” need not occur directly at a wavenumber of k_0 .

By fitting this functional form to the measured spectra, Lübken *et al.* (1993), and Lübken (1997) were able to determine ℓ'_0 to fairly high accuracy. The value of ℓ'_0 can be determined independently of C_n^2 and f_α . They then assumed that ℓ'_0 is proportional to ℓ_0 , and so used a variation on (8) viz.

$$\ell'_0 = c'_4 \eta. \quad (36)$$

They used $c'_4 = 9.90$ to get η , and thence determined ε . This choice required some knowledge about the Prandtl number, and there is some uncertainty in this regard. Lübken *et al.* (1993) and Lübken (1997) used 0.82, whilst Hill and Clifford (1978) suggest 0.72. The latter result is the correct choice if it is recognized that the temperature spectra and the neutral density spectra are identical in form. An example of the measured and fitted spectra is shown in Fig. 6.

However, it is appropriate at this juncture that we make some comments about the function $W(\omega)$. This function is designed to describe both the inertial range of the spectrum as well as the viscous range, plus the transition between them. It is proportional to ω^{-7} at large ω , which limits its usefulness to some degree. For example, if one requires the variance of the third derivative of the spatial fluctuations, (as is sometimes sought in turbulence studies), then it involves an integral over all ω of W multiplied by ω^6 , which is an integral of ω^{-1} , and is therefore infinite. Higher order derivatives have similar infinities. Indeed, Heisenberg's original proposal for a ω^{-7} form at high wavenumbers was criticized by, for example, Batchelor, for reasons like this. Furthermore, Heisenberg's formula was really only supposed to apply to energy spectra,

whereas Lübken *et al.* have adapted it to scalar spectra. The possibility of such infinite integrals places some limits on the usefulness of this particular function; if this functional form is indeed used, it is necessary that the user places some sort of artificial limit on the integrals, or assumes that the spectrum changes form yet again at some point well into the viscous range.

Indeed, the optimal choice of $W(\omega)$ requires additional discussion, and should at this stage be considered indeterminate. Lübken found by experimentally fitting the data to different functions that the so-called “Heisenberg” theoretical form described by Eqs. (34) and (35) gave the best fit, although his original papers also discussed a model due to Tatarskii (1971) for the viscous range. However, we have noted doubts about the suitability of the Heisenberg form. Another possibility which well deserves examination is the temperature spectrum of Hill and Clifford (1978). It should be recognized that within turbulence in the free air, the fluctuations in temperature and the fluctuations in density should have the same form, since neutral fluctuations due to pressure perturbations are negligible, so this is an excellent candidate. Nevertheless, for now we recognize that Lübken's preference is to use Eq. (34). We recognize that the chief new contribution from Lübken *et al.* (1993) and Lübken (1997) to measurements of turbulence was to develop a formalism whereby ℓ'_0 could be determined using *all* of the available spectrum, thereby (hopefully) producing higher accuracy.

This method was then used extensively by Lübken (1997) to determine a climatology of ε . An example will be discussed shortly in regard to Fig. 8. The method appears to be moderately reliable, although it should be emphasized that the assumption that $\ell'_0 = \ell_0$ is still unproven; this can lead to systematic errors in ε . Questions about the correct choice of

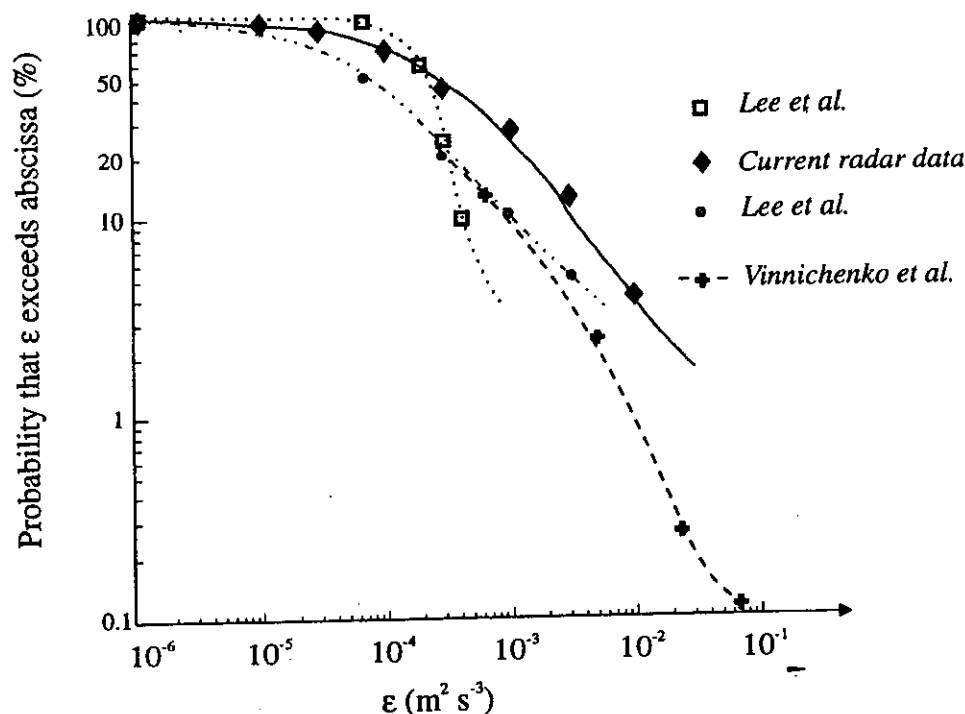


Fig. 7. Cumulative graph of ϵ in the troposphere (from Hocking and Mu, 1997), using radar data and the theory embodied in Eqs. (10) and (33), as well as various in-situ measurements. Data are compared to Lee *et al.* (1988) and Vinnichenko *et al.* (1973).

the Prandtl number have also been noted above. Additionally, because ϵ varies as the fourth power of ℓ'_0 , even small errors in estimating ℓ'_0 can lead to considerable errors in ϵ . However, even despite these problems, the method remains one of the more commonly used for rocket studies of turbulence. It is only possible to guess at the effects of these systematic errors, although we would hope that the method gives accuracies which are correct to within a factor of 2.

6.3 Application of the new C_n^2 formula to some in-situ data

In this section, we wish to intercompare the two approaches described in Subsections 6.1 and 6.2, since they have been two of the main approaches to determinations of ϵ by rocket techniques. Previous comparisons have not always shown good agreement, but in each case we have noted recent developments and adjustments, so it will be of interest to see how the two different techniques now compare after these new developments are considered.

The formulae presented in Subsection 6.1, which involve the more proper use of γ , have been tested in at least a couple of cases, and seem to produce somewhat better estimates than do those which do not properly consider the Richardson-number dependence of this quantity. We shall illustrate some of these, but it should nevertheless be borne in mind that even the tests shown here are not really definitive, and more tests are unquestionably needed. In particular, in these tests we have had to assume that $\gamma = 0.4$, whereas it would be much nicer to use actual measured values of the Richardson number made at scales of a few tens to hundreds of metres.

The first such test is shown in Fig. 7, which summarizes results from Hocking and Mu (1997), using tropospheric data. This shows a cumulative distribution of energy dissipa-

tion rates measured by various techniques, including radar. Whilst the data were taken at different sites, and on different occasions, the overall agreement is quite reasonable. Values obtained by radar and shown here, for example, show broadly better agreement than those which do not use this more recent theory.

A more interesting comparison comes about by examining the same data using two different analysis techniques. We have chosen the rocket data obtained by Thrane *et al.* (1985, 1987), Lübken *et al.* (1987), and Blix *et al.* (1990), which have been nicely tabulated in those references. We have converted the energy dissipation rates produced by these authors back to effective structure constants (analogous to C_n^2 but in this case they were ion or electron density or neutral density structure constants), and then re-determined ϵ using Eqs. (10) and (33). We used F equal to 1, because when using in-situ data there is no need to concern ourselves about an incompletely filled measuring volume—the data are recorded at very high resolution by the moving probe, and the measuring instruments have volumes much smaller than the size of any turbulent patch. We have then compared the new data to estimates of ϵ obtained by Lübken (1997) using his “spectral-knee” formalism (see the previous section). The results are shown in Fig. 8; we have concentrated on the region above 80 km altitude. The most important line is that for winter, since most of the raw data used were taken in Autumn and Winter (specifically October 1987, November 1980, January 1984 and February 1984; see references cited above). The solid circles (theory presented here-in) seem to show better agreement with Lübken (1997) than do the filled squares. Therefore it seems that data produced with the newer version of (10), using (33), provide broadly better consistency with

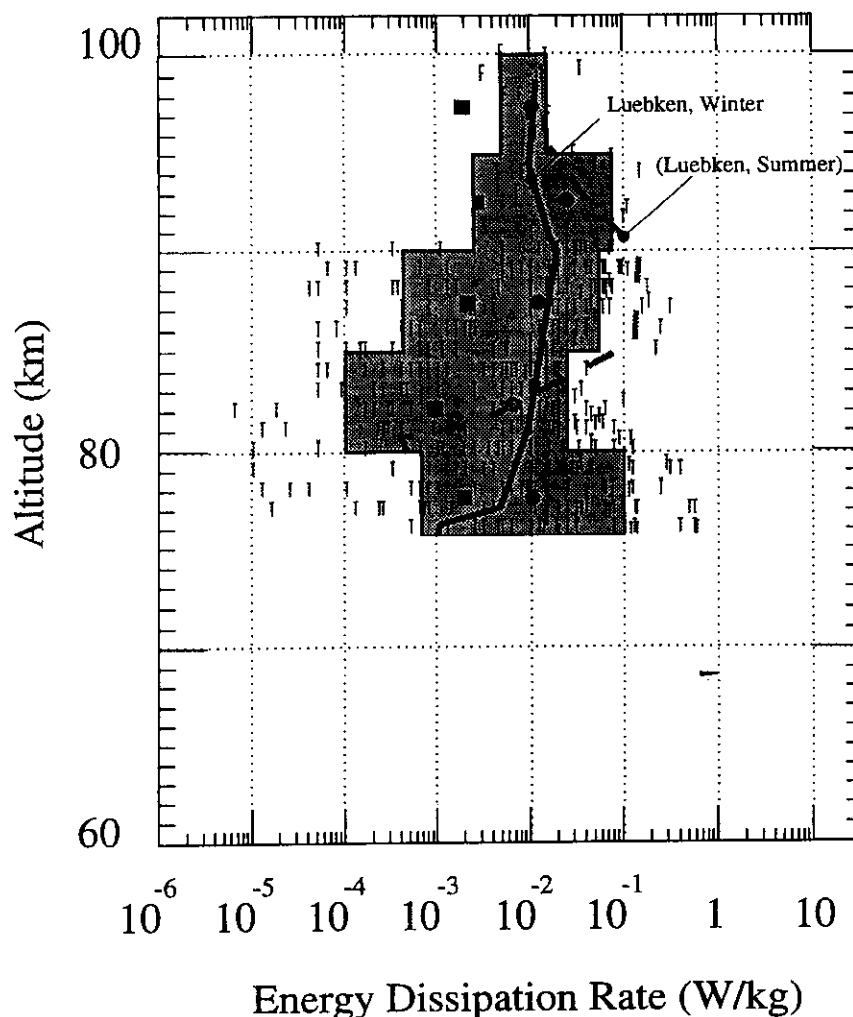


Fig. 8. Energy dissipation rates from Thrane *et al.* (1985), Lübken *et al.* (1987) and Blix *et al.* (1990), produced after rescaling according to Eqs. (10) and (33). Rescaled raw data are shown by the symbols "T". The filled squares show median values of ϵ due to the original authors, whilst the solid circles show median values using the newer theory. The left and right borders of the filled area shows 16% and 84% percentiles using the newer theory. The solid lines show estimates for summer and winter due to Lübken (1997), using his procedure for fitting spectra to the data.

the methods described in Subsection 6.2 than do the earlier methods.

7. The Relation between Diffusion and Energy Dissipation Rates

The issue of the relation between the rates of diffusion and the rate of energy dissipation in the atmosphere is another area which is often oversimplified. It is often assumed that (11) applies, and that measurements of ϵ immediately enable determination of the rate of vertical diffusion, K . Authors vary in their assumed values of c_2 , but most (with the possible exception of McIntyre, 1989) generally agree that the value lies between 0.2 and 1.25 (e.g. Fukao *et al.*, 1994; Lilly *et al.*, 1974; Weinstock, 1981). We will not dwell too much on the actual value of c_2 here; it is premature to specify it more precisely than has been done here, although a value of 0.8 is commonly used.

A more important matter here is not what c_2 is, but rather whether (11) applies at all. The methods by which diffusion can take place are far more complex than simple three-dimensional turbulent diffusion. The reasons for this lie in

two main facts; first, turbulence is very intermittent both temporally and spatially, and very often occurs in thin layers in the middle atmosphere. These thin layers are often separated by regions which are either only weakly turbulent or even laminar. Secondly, the processes which induce diffusion can themselves be scale dependent.

These factors mean that there are several ways in which diffusion can occur. Table I summarizes some of these processes, and we will now elaborate briefly upon them.

The first important factor is the spatial and temporal intermittency. This effect has been demonstrated in Hocking (1991, 1996b), after adaptation from Desaubies and Smith (1982). These authors show how an ensemble of gravity waves can act together to produce regions of instability separated in height by regions of stability, with layer thicknesses of a few tens of metres out to a kilometre or so. Examples of experimental studies of such layering are also discussed there-in.

The consequences of this intermittency are important. They mean, for example, that we must revisualize how large-scale turbulent diffusion takes place. An important proposal

Table 1. This table shows some of the various processes which are normally grouped together as "diffusive" processes in the atmosphere. Classical turbulent diffusion is only one such process, and at large scales is not necessarily even one of the most important. At intermediate scales (500 m to 3 km), all of these processes occur, but we have left question marks here to indicate that it is uncertain just which of all these processes dominates in this regime.

Scale	Momentum	Constituents/temperature
<500 m	$K \propto \frac{\epsilon}{\omega_b^2}$	$K \propto \frac{\epsilon}{\omega_b^2}$
500 m to 3 km	all processes described above and below— but which dominates?	all processes described above and below— but which dominates?
>3 km	"Classical turbulent diffusion" Stochastic Layering Quasi-horizontal diffusion (Slant-wise convection) + other?	"Classical turbulent diffusion" Stochastic Layering Quasi-horizontal diffusion (Slant-wise convection) Stokes Diffusion + other?

due to Dewan (1981) and Woodman and Rastogi (1984) suggested that the random occurrence of layers produces a Monte Carlo type of intermittent diffusion. In this model, diffusion is not a continuous process, but a step-wise one. First one layer of turbulence forms around a particle of interest, purely due to chance. Turbulent transport of this particle then takes place, possibly to the edge of the layer, or until the layer dies out. At this time the particle remains fairly stationary, since molecular diffusion is assumed to be very small. Then at a later time, another turbulent layer forms around the particle, and further transport over the depth of that layer is now possible. This process repeats itself over and over. Thus the factors which control the large-scale diffusion are not simply the rates of diffusion across individual layers, but the frequency of occurrence and depth of individual layers (this process is illustrated diagrammatically in Fig. 2 of Hocking, 1991). Any determinations of effective diffusion coefficients must take this into account. Proper modelling of the effects of this intermittency remains an important area of research.

Other consequences of the intermittency of turbulence include the possibility that the average rates of diffusivity of momentum and heat may be different, and that the Prandtl number may exceed 1, and perhaps be in the range of 1 to 3 (Fritts and Dunkerton, 1985). This is to say that if one parameterizes the rate of heat transport as $K_T(\partial\bar{\theta}/\partial z)$, where $\partial\bar{\theta}/\partial z$ is the mean potential temperature gradient, ignoring the effects of the wave, then the effective coefficient which must be used to describe the rate of diffusion is less than it would be if we properly included the effect of the wave in $\partial\bar{\theta}/\partial z$. This is not so for momentum diffusion, because 'u' and 'w' are not in phase quadrature. Fritts and Dunkerton (1985) have proposed this process as a way to explain the conclusions of Strobel *et al.* (1987), in which these authors claim that the turbulent Prandtl number is somewhat in excess of unity in the atmosphere.

Another important means of vertical diffusion is quasi-horizontal diffusion along tilted isopleths. It is well known that horizontal diffusion at large scales is a much faster pro-

cess than vertical diffusion. If the mean gradients are tilted, then this horizontal diffusion attains a vertical component, and can lead to an effective vertical mixing. Admittedly a particle which starts at an altitude of z km, and finally achieves a height of $z + \zeta$ km, may also have drifted horizontally a distance equal to perhaps hundreds of times ζ , but nevertheless this still produces an effective vertical mixing.

Another important process which can produce significant diffusion is so-called "Stokes Diffusion", as proposed by Walterscheid and Hocking (1991) and Hocking and Walterscheid (1993). These authors have shown that even a linear combination of Boussinesq waves produces a diffusive-like effect on particles over periods of many hours, and whilst this process is not as strong as classical turbulence in causing diffusion at scales of a few tens to hundreds of metres, it becomes a major diffusive effect when applied at scales of many hours. This is because it is not affected by the intermittency of turbulence, and acts just as strongly in laminar regions as it does in turbulent ones. This process is especially important for diffusion of constituents. If the waves are damped, the diffusive effect becomes even stronger, especially if the damping induces particles to cross between contours of constant potential temperature; in this case, Stokes diffusion may also be important for momentum diffusion. As noted, Table 1 summarizes some of these processes.

Therefore we conclude this section by simply noting that the relation between rates of diffusion and energy dissipation is not simple, and in fact is both scale and species dependent. This is still an area which deserves much research, and the key point to note is that previous visualizations and parameterizations of these processes have been grossly oversimplified in the past. Diffusion is scale dependent, and the types of diffusion coefficients which a global-scale modeller might use may be very different (usually larger) than the ones which might be needed to describe small scale mixing in the atmosphere.

8. Conclusion

Some of the constants traditionally used in turbulence theory, and indeed some classical interpretations, have been re-examined. The basis for these formulae have been discussed, showing how some of these constants arise. Appropriate formulae for application of radar and in-situ measurements of turbulence have been presented, including recommendations for the most appropriate constants where possible. Where necessary, oversimplifications in current thinking about turbulence have also been pointed out. Without question, though, all current measurements of energy dissipation rates in the middle atmosphere have uncertainties of some type; a major goal in the next few years should be to develop instrumentation which can directly measure velocity fluctuations in-situ down to scales within the viscous range. Only then will it be possible to unambiguously interpret the spectra, and determine turbulent energy dissipation rates with precision.

Acknowledgments. The careful comments and suggestions of two anonymous reviewers were of great help in the final preparation of this document. This work was supported in part by the Natural Sciences and Engineering Research Council of Canada.

Appendix A. Velocity Structure Functions

The following appendices summarize the main structure functions and spectra used in turbulence theory, without proof or derivation.

The first type of function which we will discuss that is commonly used to describe turbulent phenomena is the so-called Structure Function. There are several of these, but the main ones are D_{\parallel} and D_{\perp} , which are defined in the following way;

$$D_{\parallel}(r) = |\overline{u_{\parallel}(\underline{x} + \underline{r})} - \overline{u_{\parallel}(\underline{x})}|^2 \quad (\text{A.1})$$

and

$$D_{\perp}(r) = |\overline{u_{\perp}(\underline{x} + \underline{r})} - \overline{u_{\perp}(\underline{x})}|^2, \quad (\text{A.2})$$

where we imagine traversing the turbulent medium in a straight line and taking point measurements along the way. "Parallel" components refer to measurements of the velocity components with directions parallel to the direction of traverse, and "perpendicular" components refer to velocity components perpendicular to this direction. Isotropy has been assumed in this definition, which is why we consider D to depend only on the magnitude r of the vector \underline{r} .

Occasionally a 3-D form of the structure function is sometimes used, viz.

$$D_{\text{tot}}(r) = |\overline{\underline{u}(\underline{x} + \underline{r})} - \overline{\underline{u}(\underline{x})}|^2, \quad (\text{A.3})$$

where the vector difference between displaced components is used. Because there are two perpendicular components, and one parallel component, we may write

$$D_{\text{tot}} = D_{\parallel} + 2D_{\perp}. \quad (\text{A.4})$$

For inertial range, homogeneous, Kolmogoroff-style turbulence, we have the following relations.

$$D_{\parallel} = C_v^2 r^{2/3} \quad (\text{A.5})$$

where $C_v^2 = C\varepsilon^{2/3}$, and C is close to 2.0 (e.g. Caughey *et al.*, 1978; Kaimal, 1976). In addition,

$$D_{\perp} = \frac{4}{3} C_v^2 r^{2/3}, \quad (\text{A.6})$$

$$D_{\text{tot}} = \frac{11}{3} C_v^2 r^{2/3}. \quad (\text{A.7})$$

There are also a variety of spectral forms which are used as tools in turbulence studies.

Appendix B. Spectral Forms for Velocity Measurements

A variety of spectra are used for turbulence studies. These all have different purposes, and are summarized below for Kolmogoroff-type inertial-range turbulence.

The first important expression is

$$\mathcal{F}(\underline{k}) \doteq A\varepsilon^{2/3} k^{-11/3} \quad (\text{B.1})$$

where $k = |\underline{k}|$ is the length of the vector \underline{k} , (and so takes values between 0 and infinity), and $A = \frac{11\Gamma(\frac{5}{6})\sin(\frac{\pi}{6})}{24\pi^2} C \simeq 0.061C$, (Tatarskii, 1971). This is a full three-dimensional function describing the total kinetic energy per unit cell size (due to all three velocity components) in a cell of size d^3k at the end of a vector \underline{k} originating from the origin. For homogeneous isotropic turbulence this function is isotropic. Pictorially one can visualize this as a solid sphere in (k_x, k_y, k_z) -space which has highest density at the centre, and decreasing density as $|k|$ increases, where the density represents \mathcal{F} .

Because this function is isotropic, it is often integrated over a shell of radius k to give a new expression which is

$$E(k) = 4\pi k^2 \mathcal{F} = \alpha \varepsilon^{2/3} k^{-5/3} \quad (\text{B.2})$$

where $\alpha = 4\pi A = \frac{11\Gamma(\frac{5}{6})\sin(\frac{\pi}{6})}{6\pi} C = 0.76655C$ (e.g. see Tatarskii, 1971; Batchelor, 1953). Note that we will largely follow Batchelor's symbol-usage in this document: For example, we use $E(k)dk$ to represent the total energy in a shell in k -space of thickness dk , as does Batchelor, whereas Tatarskii (1961, 1971) uses the symbol E to represent the function which we have called \mathcal{F} .

If we use $C = 2.0$, then we have

$$E(k) = 1.53\varepsilon^{2/3} k^{-5/3}. \quad (\text{B.3})$$

Different authors use different values for the constant 1.53—anything between 1.35 and 1.53 are common. Note, however, that if one adjusts this constant then the constant C also needs adjustment. I prefer to use $C = 2.0$ because it has at least been measured with good accuracy in the lower atmosphere (e.g. Caughey *et al.*, 1978).

These equations are fairly simple to understand. However, there are more complex variants. An important adjunct (and in fact a more fundamental expression) is the equation

$$\Phi_{ij}(\underline{k}) = \frac{E(k)}{4\pi k^4} \cdot (k^2 \delta_{ij} - k_i k_j) \quad (\text{B.4})$$

which describes the three-dimensional cross-spectrum between the velocity components in the "i" direction and the "j" direction, where "i or j = 1" mean the x direction, "i

or $j = 2$ mean the y direction and " i or $j = 3$ " mean the z direction. The values k_1, k_2 and k_3 may take both positive and negative values. Note that k is the length of the vector from the origin to the point (k_1, k_2, k_3) in k -space, and so $k^2 = k_1^2 + k_2^2 + k_3^2$.

For each of these spectra there is a related covariance function; for example,

$$\Phi_{it}(\underline{k}) = \frac{1}{8\pi^3} \int_{-\infty}^{\infty} \int_{-\infty}^{\infty} \int_{-\infty}^{\infty} e^{-j\underline{k} \cdot \underline{\xi}} R_{it}(\underline{\xi}) d\underline{\xi} \quad (\text{B.5})$$

where R_{it} is the autocovariance function corresponding to Φ_{it} and where $j = \sqrt{-1}$ in this expression. We will not discuss these various covariance functions in much detail here; the reader is referred to Tatarskii (1961, 1971), Batchelor (1953) or Lumley and Panofsky (1964) for more elaborate discussions.

For cases of isotropic turbulence, we can integrate Φ_{ij} around a shell of radius k to give (e.g. Batchelor, 1953, p. 35)

$$\Psi_{ij}(k) = \oint \Phi_{ij}(\underline{k}) k^2 d\Omega_k. \quad (\text{B.6})$$

For homogeneous, isotropic turbulence, we therefore have

$$\Psi_{ij}(k) = 4\pi k^2 \Phi_{ij}(k). \quad (\text{B.7})$$

$E(k)$ relates to the Ψ_{ij} (and hence to the Φ_{ij}) via the relation

$$E(k) = \frac{1}{2} (\Psi_{11}(k) + \Psi_{22}(k) + \Psi_{33}(k)). \quad (\text{B.8})$$

Notice the factor $\frac{1}{2}$; this is introduced so that the integral over all k (i.e. from $k = 0$ to $k = \infty$) gives the kinetic energy per unit mass, $\frac{1}{2} \overline{u_{10}^2}$. $E(k)$ is unique in this regard—other spectra have normalizations which do not involve this factor of $\frac{1}{2}$. For example,

$$\int_0^{\infty} \Psi_{11}(k) dk = \overline{u_1^2} \quad (\text{B.9})$$

where u_1 refers to the velocity component in the x direction.

Sometimes (B.8) is also written as

$$E(k) = \frac{1}{2} \oint_{k_1 k_2 k_3 = k^2} \Phi_{ii}(\underline{k}) k^2 d\Omega_k. \quad (\text{B.10})$$

where the subscript ' ii ' means sum the three terms Φ_{11} , Φ_{22} and Φ_{33} (e.g. Lumley and Panofsky, 1964, p. 28).

The above spectra are useful from a conceptual viewpoint, but are often hard to determine experimentally, since they require a full three-dimensional description of the turbulent field in all three velocity components. That is, they require knowledge of all three velocity components at all points in space. This is often difficult (if not impossible) to measure.

Therefore, we also look for spectral analogues to the structure functions which were described earlier for a one-dimensional pass through the turbulent field.

To begin, if we have a detector which moves in a straight line through a patch of turbulence, and it records the velocity components parallel to the direction of motion (in analogy to the process described in connection with Eqs. (A.1) to (A.3)),

and then we Fourier transform the resultant spatial series, we obtain (for Kolmogoroff turbulence) the function

$$\Theta_{11}(k_1, 0, 0) = \alpha'_{11} \varepsilon^{2/3} |k_1|^{-5/3} \quad (\text{B.11})$$

where $\alpha'_{11} = \frac{9}{55} \alpha = 0.1244C$. This is in fact a one-dimensional function which we will denote as ϕ_p , viz.

$$\phi_p(k_1) = \alpha'_{11} \varepsilon^{2/3} |k_1|^{-5/3}. \quad (\text{B.12})$$

It is important to note that this is *not* the same as $\Phi_{11}(k_1, 0, 0)$. Whilst both refer to spectral densities along the x axis, $\Phi_{11}(k_1, 0, 0)$ refers to spectral densities due *only* to "waves" with the phase-fronts aligned perpendicular to the x axis. On the other hand, $\Theta_{11}(k_1, 0, 0)$ (and $\phi_p(k_1)$) refer to the spectral density at wavenumber k_1 due to contributions of "waves" of *all* orientations which cross the x axis. These concepts are fundamentally different. In fact,

$$\Theta_{ij}(k_1, 0, 0) = \iint \Phi_{ij}(k_1, k_2, k_3) dk_2 dk_3. \quad (\text{B.13})$$

Likewise, if we find the spectrum for the velocity components perpendicular to the direction of motion during this traverse, we produce

$$\phi_t(k_1) = \Theta_{22}(k_1, 0, 0) = \alpha'_{22} \varepsilon^{2/3} |k_1|^{-5/3} \quad (\text{B.14})$$

where $\alpha'_{22} = \frac{4}{3} \alpha'_{11}$.

Additionally, for the choice of $C = 2.0$ described above, we have

$$\phi_p(k_1) = \Theta_{11}(k_1, 0, 0) = 0.25 \varepsilon^{2/3} |k_1|^{-5/3} \quad -\infty < k_1 < \infty, \quad (\text{B.15})$$

$$\phi_t(k_1) = \Theta_{22}(k_1, 0, 0) = 0.33 \varepsilon^{2/3} |k_1|^{-5/3} \quad -\infty < k_1 < \infty. \quad (\text{B.16})$$

In the case of isotropic turbulence, there is no preferred axis, so that these formulae are not restricted to any particular axis.

Because of the obvious symmetry, many experimentalists often "fold" their spectral densities at negative wavenumbers over onto their positive ones, and so do not differentiate between positive and negative signs for the wavenumber. Then we obtain the following functions:

$$\phi'_p(k_\alpha) = 0.50 \varepsilon^{2/3} k_\alpha^{-5/3} \quad 0 < k_\alpha < \infty, \quad (\text{B.17})$$

$$\phi'_t(k_\alpha) = 0.67 \varepsilon^{2/3} k_\alpha^{-5/3} \quad -\infty < k_\alpha < \infty \quad (\text{B.18})$$

where k_α are absolute values of wavenumbers along the direction of travel of the probe.

Note that Eqs. (B.11), (B.12), (B.14), and (B.15) to (B.18), have " $k^{-5/3}$ " laws, but so does (B.2). However, these equations are conceptually different; (B.2) represents an integration over a shell of radius k in three-dimensional k -space, whilst (B.15) to (B.18) represent spectra determined by a probe moving in a straight line through the turbulence. Nevertheless, it is a common mistake for novice researchers to confuse the two spectra, when they speak of the " $k^{-5/3}$ " law, which can lead to the propagation of considerable confusion. It is important to conceptually distinguish these spectra.

Appendix C. Scalar Structure Functions and Spectra

In some studies of turbulence, it is not information about the velocity fluctuations which are sought, but rather density fluctuations associated with certain tracers. One must be careful to choose a "good" tracer—certainly quantities which react chemically with their surrounds will not obey the following equations (e.g. see Hocking, 1985).

The structure function is described as

$$D_\zeta(r) = \overline{[\zeta(\underline{x} + \underline{r}) - \zeta(\underline{x})]^2} \quad (\text{C.1})$$

where ζ represents the scalar concentration. For Kolmogoroff inertial range turbulence this is given by

$$D_\zeta(r) = C_\zeta^2 r^{2/3}. \quad (\text{C.2})$$

The first important spectral form is $\Phi_\zeta(k)$, which is the full three-dimensional spectral density function. For Kolmogoroff turbulence, it is given by

$$\Phi_\zeta(k) = 0.033 C_\zeta |k|^{-11/3} \quad (\text{C.3})$$

in the inertial range. The nearest analogy to this spectrum for the velocity case is the function \mathcal{F} from Eq. (B.1); Φ_ζ should not be confused with Φ_{ij} from Eq. (B.4), although the notations look similar. This convention may seem just a little confusing, but is maintained here as a result of historical precedent.

This function has been chosen to be normalized so that

$$\int_{-\infty}^{\infty} \int_{-\infty}^{\infty} \int_{-\infty}^{\infty} \Phi_\zeta(k) dk = \overline{(\zeta')^2}. \quad (\text{C.4})$$

Then for locally isotropic, homogeneous we define

$$E_\zeta(k) = 4\pi k^2 \Phi_\zeta(k) \quad (\text{C.5})$$

or

$$E_\zeta(k) = 0.132\pi C_\zeta^2 |k|^{-5/3} = 0.415 C_\zeta^2 |k|^{-5/3}. \quad (\text{C.6})$$

The function E_ζ is very analogous to the function E in Eq. (B.2).

Finally, we present the spectrum seen if we record along a straight line. This is the spectrum which a probe moving through a patch of turbulence would measure, and is very similar to ϕ_p from Eqs. (B.12) and (B.14) in the section on velocity spectra. This is given by

$$S_\zeta(k_1) = \int_{-\infty}^{\infty} \int_{-\infty}^{\infty} \Phi_\zeta(k) dk_2 dk_3 \quad (\text{C.7})$$

which, for the case of Kolmogoroff turbulence, becomes

$$S_\zeta(k) = 0.125 C_\zeta^2 |k|^{-5/3} \quad -\infty < k < \infty. \quad (\text{C.8})$$

The function S_ζ has strong similarities with ϕ_p in Eq. (B.15). If we fold negative wavenumbers onto positive, we obtain

$$S'_\zeta(k) = 0.25 C_\zeta^2 k^{-5/3} \quad 0 < k < \infty. \quad (\text{C.9})$$

Again (as for the velocity spectra), note that (C.6) and (C.9) both involve a " $k^{-5/3}$ " law, but the spectra are conceptually different.

Appendix D. C_n^2 and ϵ

The energy dissipation rate is related to the potential refractive index structure constant by

$$\bar{\epsilon} = \left(\gamma \overline{C_n^2} \frac{\omega_B^2}{F^{1/3}} M^{-2} \right)^{3/2} \quad (\text{D.1})$$

where ω_B is the Väisälä-Brunt frequency. The parameter F represents the fraction of the radar volume which is filled by turbulence, while γ is discussed in more detail in the main body of the text.

The "potential refractive index gradient" is given in the troposphere and stratosphere by

$$M = -77.6 \times 10^{-6} \frac{P}{T} \left(\frac{\partial \ln \theta}{\partial z} \right) \times \left[1 + \frac{15500q}{T} \left(1 - \frac{1}{2} \frac{\partial \ln q / \partial z}{\partial \ln \theta / \partial z} \right) \right] \quad (\text{D.2})$$

where z is height, θ is the potential temperature, q is the specific humidity, T is the absolute temperature and P is the atmospheric pressure in millibars. The term in square brackets was denoted as χ by Van Zandt *et al.*, 1978; indeed this particular form of the equation was first introduced by these authors. Note that χ tends to 1 as the humidity terms tend to zero.

In the ionosphere, where humidity is no longer important but electron density plays a crucial role, we have

$$M = \frac{\partial n}{\partial N} \left[\frac{N}{\theta} - \frac{dN}{dz} + \frac{N}{\rho} \cdot \frac{d\rho}{dz} \right] \quad (\text{D.3})$$

where again we have used the symbol θ for potential temperature and N is the electron density. The term ρ is the neutral density. The function $\frac{\partial n}{\partial N}$ needs to be determined from electro-ionic theory (e.g. Sen and Wyller, 1960; Budden, 1965; Hocking and Vincent, 1982).

References

- Barat, J., Some characteristics of clear air turbulence in the middle stratosphere, *J. Atmos. Sci.*, **39**, 2553–2564, 1982.
- Batchelor, G. K., *The Theory of Homogeneous Turbulence*, 197 pp., Cambridge University Press, New York, 1953.
- Batchelor, G. K., *An Introduction to Fluid Dynamics*, 615 pp., Cambridge University Press, Cambridge, New York, 1967.
- Blix, T. A., In-situ studies of turbulence and mixing; problems and questions, in *Coupling Processes in the Lower and Middle Atmosphere*, Vol. 387, edited by E. V. Thrane, T. A. Blix and D. C. Fritts, NATO ASI series C, pp. 329–344, Kluwer Academic Publishers, 1993.
- Blix, T. A., E. V. Thrane, and O. Andreassen, In situ measurements of the fine-scale structure and turbulence in the mesosphere and lower thermosphere by means of electrostatic positive ion probes, *J. Geophys. Res.*, **95**, 5533–5548, 1990.
- Bohne, A. R., *Radar Detection of Turbulence in Thunderstorms*, 62 pp., Report # AFGL-TR-81-0102 (ADA 108679), Air Force Geophys. Lab., Hanscom Air Force Base, MS, U.S.A., 1981.
- Bohne, A. R., Radar detection of turbulence in precipitation environments, *J. Atmos. Sci.*, **39**, 1819–1837, 1982.
- Budden, K. G., Effect of electron collisions on the formulas of magnetoionic theory, *Radio Sci.*, **69D**, 191–211, 1965.
- Caughey, S. J., B. A. Crease, D. N. Asimakopoulos, and R. S. Cole, Quantitative bistatic acoustic sounding of the atmospheric boundary layer, *Q. J. R. Meteorol. Soc.*, **104**, 147–161, 1978.
- Crane, R. K., A review of radar observations of turbulence in the lower stratosphere, *Radio Sci.*, **15**, 177–193, 1980.
- Desaubies, Y. and W. K. Smith, Statistics of Richardson number and instability in oceanic internal waves, *J. Phys. Oceanography*, **12**, 1245–1259, 1982.

- Dewan, E. M., Turbulent vertical transport due to thin intermittent mixing layers in the stratosphere and other stable fluids, *Science*, **211**, 1041–1042, 1981.
- Doviak, R. J. and D. S. Zmric, *Doppler Radar and Weather Observations*, 458 pp., Academic Press, Orlando, FL, 1984.
- Fritts, D. C. and T. J. Dunkerton, Fluxes of heat and constituents due to convectively unstable gravity waves, *J. Atmos. Sci.*, **42**, 549–556, 1985.
- Fukao, S., M. D. Yamanaka, N. Ao, W. K. Hocking, T. Sato, M. Yamamoto, T. Nakamura, T. Tsuda, and S. Kato, Seasonal variability of vertical eddy diffusivity in the middle atmosphere, 1. Three-year observations by the middle and upper atmosphere radar, *J. Geophys. Res.*, **99**, 18973–18987, 1994.
- Gage, K. S., J. L. Green, and T. E. VanZandt, Use of Doppler radar for the measurement of atmospheric turbulence parameters from the intensity of clear air echoes, *Radio Sci.*, **15**, 407–416, 1980.
- Gossard, E. E. and A. S. Frisch, Relationship of the variances of temperature and velocity to atmospheric static stability—application to radar and acoustic sounding, *J. Clim. Appl. Meteorol.*, **26**, 1021–1036, 1987.
- Gossard, E. E., R. B. Chadwick, W. D. Neff, and K. P. Moran, The use of ground-based Doppler radars to measure gradients, fluxes and structure parameters in elevated layers, *J. Appl. Meteorol.*, **21**, 211–226, 1982.
- Gossard, E. E., R. B. Chadwick, T. R. Detman, and J. Gaynor, Capability of surface-based clear-air Doppler radar for monitoring meteorological structure of elevated layers, *J. Clim. Appl. Meteorol.*, **23**, 474–485, 1984.
- Gossard, E. E., J. Gaynor, R. J. Zamora, and W. D. Neff, Fine structure of elevated stable layers observed by sonder and in-situ tower sensors, *J. Atmos. Sci.*, **42**, 2156–2169, 1985.
- Hill, R. J. and S. F. Clifford, Modified spectrum of atmospheric temperature fluctuations and its application to optical propagation, *J. Opt. Soc. Am.*, **68**, 892–899, 1978.
- Hocking, W. K., On the extraction of atmospheric turbulence parameters from radar backscatter Doppler spectra—I: theory, *J. Atmos. Terr. Phys.*, **45**, 89–102, 1983.
- Hocking, W. K., Measurement of turbulent energy dissipation rates in the middle atmosphere by radar techniques: a review, *Radio Sci.*, **20**, 1403–1422, 1985.
- Hocking, W. K., Observation and measurement of turbulence in the middle atmosphere with a VHF radar, *J. Atmos. Terr. Phys.*, **48**, 655–670, 1986.
- Hocking, W. K., The effects of middle atmosphere turbulence on coupling between atmospheric regions, *J. Geomag. Geoelectr.*, **43**, 621–636, 1991.
- Hocking, W. K., On the relationship between the strength of atmospheric radar backscatter and the intensity of atmospheric turbulence, *Adv. Space Res.*, **12**(10), 207–213, 1992.
- Hocking, W. K., An assessment of the capabilities and limitations of radars in measurements of upper atmosphere turbulence, *Adv. Space Res.*, **17**(11), 37–47, 1996a.
- Hocking, W. K., Small scale dynamics of the upper atmosphere: experimental studies of gravity waves and turbulence, chapter 1.2.2 (invited) in *The Upper Atmosphere*, edited by W. Dieminger, G. K. Hartmann, and R. Leitinger, pp. 51–96, Springer-Verlag, Berlin, Heidelberg, New York, 1996b.
- Hocking, W. K. and A. M. Hamza, A Quantitative measure of the degree of anisotropy of turbulence in terms of atmospheric parameters, with particular relevance to radar studies, *J. Atmos. Sol.-Terr. Phys.*, **59**, 1011–1020, 1997.
- Hocking, W. K. and K. L. Mu, Upper and Middle Tropospheric Kinetic Energy Dissipation Rates from Measurements of C_n^2 —Review of Theories, in-situ Investigations, and Experimental Studies using the Buckland Park Atmospheric Radar in Australia, *J. Atmos. Terr. Phys.*, **59**, 1779–1803, 1997.
- Hocking, W. K. and R. A. Vincent, Comparative observations of D-region HF partial reflections at 2 and 6 MHz, *J. Geophys. Res.*, **87**, 7615–7624, 1982.
- Hocking, W. K. and R. L. Walterscheid, The role of Stokes' diffusion in middle atmospheric transport, NATO (North Atlantic Treaty Organization) publication in *Coupling Processes in the Lower and Middle Atmosphere*, (Series C: Mathematical and Physical Sciences, Vol. 387), edited by E. V. Thrane, T. A. Blix, and D. C. Fritts, pp. 305–328, Kluwer Academic Publishers, Dordrecht, Boston and London, 1993.
- Kaimal, J. C., J. C. Wyngaard, D. A. Haugen, O. R. Cote, Y. Izumi, S. J. Caughey, and C. J. Readings, Turbulence structure in the convective boundary layer, *J. Atmos. Sci.*, **33**, 2152–2168, 1976.
- Labitt, M., Some basic relations concerning the radar measurement of air turbulence, Mass. Inst. of Technol., Lincoln Lab., Work. Pap. 46WP-5001, 1979.
- Lee, Y., A. R. Paradis, and D. Klinge-Watson, Preliminary Results of the 1983 coordinated aircraft-Doppler weather radar turbulence experiment, volume I, Report # DOT/FAA/PM-86/11 (A197894), 76 pp., Lincoln Lab., MIT, Lexington, Mass., U.S.A., 1988.
- Lilly, D. K., D. E. Waco, and S. I. Adelfang, Stratospheric mixing estimated from high-altitude turbulence measurements, *J. Appl. Meteorol.*, **13**, 488–493, 1974.
- Lübken, F.-J., Seasonal variation of turbulent energy dissipation rates at high latitudes as determined by in situ measurements of neutral density fluctuations, *J. Geophys. Res.*, **102**, 13441–13456, 1997.
- Lübken, F.-J., U. Von Zahn, E. V. Thrane, T. Blix, G. A. Kokin, and S. V. Pachomov, In-situ measurements of turbulent energy dissipation rates and eddy diffusion coefficients during MAP/WINE, *J. Atmos. Terr. Phys.*, **49**, 763–776, 1987.
- Lübken, F.-J., W. Hillert, G. Lehmacher, and U. von Zahn, Experiments revealing small impact of turbulence on the energy budget of the mesosphere and lower thermosphere, *J. Geophys. Res.*, **98**, 20369–20384, 1993.
- Lumley, J. L. and H. A. Panofsky, *The Structure of Atmospheric Turbulence*, 239 pp., John Wiley and Sons, New York, London, Sydney, 1964.
- McIntyre, M. E., On dynamics and transport near the polar mesopause in summer, *J. Geophys. Res.*, **94**, 14617–14628, 1989.
- Nastrom, G. D., Doppler radar spectral width broadening due to beamwidth and wind shear, *Ann. Geophys.*, **15**, 786–796, 1997.
- Ottersten, H., Atmospheric structure and radar backscattering in clear air, *Radio Sci.*, **4**, 1179–1193, 1969.
- Sen, H. K. and A. A. Wyller, On the generalization of the Appleton-Hartree magnetoionic formulas, *J. Geophys. Res.*, **65**, 3931–3950, 1960.
- Strobel, D. F., M. E. Summers, R. M. Bevilacqua, M. T. DeLand, and M. Allen, Vertical constituent transport in the mesosphere, *J. Geophys. Res.*, **92**, 6691–6698, 1987.
- Tatarskii, V. I., *Wave Propagation in a Turbulent Medium*, 285 pp., McGraw-Hill, New York, 1961.
- Tatarskii, V. I., *The Effects of the Turbulent Atmosphere on Wave Propagation*, 472 pp., Keter Press, Jerusalem, 1971.
- Thrane, E. V., Ø. Andreassen, T. Blix, B. Grandal, A. Brekke, C. R. Philbrick, F. J. Schmidlin, H. U. Widdel, U. Von Zahn, and F.-J. Lübken, Neutral air turbulence in the upper atmosphere observed during the Energy Budget Campaign, *J. Atmos. Terr. Phys.*, **47**, 243–264, 1985.
- Thrane, E. V., T. A. Blix, C. Hall, T. L. Hansen, U. von Zahn, W. Meyer, P. Czechowsky, G. Schmidt, H.-U. Widdel, and A. Neumann, Small scale structure and turbulence in the mesosphere and lower thermosphere at high latitudes in winter, *J. Atmos. Terr. Phys.*, **49**, 751–762, 1987.
- Van Zandt, T. E., J. L. Green, K. S. Gage, and W. L. Clark, Vertical profiles of refractivity turbulence structure constant: Comparison of observations by the Sunset radar with a new theoretical model, *Radio Sci.*, **13**, 819–829, 1978.
- Van Zandt, T. E., K. S. Gage, and J. M. Warnock, An improved model for the calculation of profiles of and in the free atmosphere from background profiles of wind, Temperature and humidity, paper presented at 20th Conference on Radar Meteorology, Am. Met. Soc., Boston, Mass., Nov. 30–Dec. 3, 1981.
- Vinnichenko, N. K., N. Z. Pinus, S. M. Shmater, and G. N. Shur, *Turbulence in the Free Atmosphere* (translated from Russian, translations editor J. A. Dutton), 263 pp., Consultants Bureau, NY, London, 1973.
- Walterscheid, R. L. and W. K. Hocking, Stokes diffusion by atmospheric internal gravity waves, *J. Atmos. Sci.*, **48**, 2213–2230, 1991.
- Watkins, B. J., C. R. Philbrick, and B. B. Balsley, Turbulence energy dissipation rates and inner scale sizes from rocket and radar data, *J. Geophys. Res.*, **93**, 7009–7014, 1988.
- Weinstock, J., On the theory of turbulence in the buoyancy subrange of stably stratified flows, *J. Atmos. Sci.*, **35**, 634–649, 1978a.
- Weinstock, J., Vertical turbulent diffusion in a stably stratified fluid, *J. Atmos. Sci.*, **35**, 1022–1027, 1978b.
- Weinstock, J., Using radar to estimate dissipation rates in thin layers of turbulence, *Radio Sci.*, **16**, 1401–1406, 1981.
- Woodman, R. F. and P. K. Rastogi, Evaluation of effective eddy diffusive coefficients using radar observations of turbulence in the stratosphere, *Geophys. Res. Letts.*, **11**, 243–246, 1984.

Because I have included the previous paper, I also include an extract from the following paper by Roper.

The equations shown at (*) by Roper were derived largely by dimensional analysis, and so the "equations" are not really equalities. They should more properly be written as " \sim " or "of the order of".

One needs to ^{take} great care in interpreting "equalities" in the literature in regard to turbulence.


Equation (28) in the previous paper,


$$\text{viz } \epsilon = 0.47 \sigma^2 \omega_B \quad (28)$$

$$\text{and (29) } \epsilon = 0.47 \sigma^2 \omega_B \left(\frac{1}{C_F} \right)^{\frac{2}{3}} \quad (29)$$

were derived from quite rigorous physical argument. In contrast, equation (4) from Roper gives

$$\epsilon = 0.16 \sigma^2 \omega_B.$$

The derivation ~~of~~ of this equation was dimensional, and also suffered from one other limitation. This is the fact that Roper used an autocovariance approach to estimate an RMS velocity, but then ascribes these velocities as being related to an integral associated with the spectrum. As shown by Hocking (1983, JATP) - also see the extract 2 pages on ^{from here} the autocovariance estimate σ^2 is not just the shaded section , but also

2, 8
includes the "dotted" section () This alters the
"constant", and so Roper's " σ " is NOT the same as
the " σ " in equations (28) & (29).

Thus not only is it inappropriate to
compare the "constants" of 0.47 & 0.16, but it
is also inappropriate to consider the " σ " values
as the same. Notice that the difference between (18) & (20)
3 pages on from here is a factor of 3.5: $(0.47/0.16) \approx 3.0$

Care about things like the meaning
of various terms, and consideration about
the precision used in the calculations (eg is
it ~~proper~~ dimensional analysis, or more
rigorous?) are necessary before you can
decide on the validity of the constants in
many of these expressions

On the radar estimation of turbulence parameters in a stably stratified atmosphere

R. G. Roper

School of Earth and Atmospheric Sciences, Georgia Institute of Technology, Atlanta

Abstract. Four estimators of the rate of dissipation of turbulent energy based on the velocity structure function, rms turbulent velocities, Brunt-Väisälä frequencies, and ground diffraction pattern fading rates are discussed and compared using Arecibo Initiative on the Dynamics of the Atmosphere MF radar data in both the imaging Doppler interferometry (IDI) and spaced antenna modes. A consistent set of empirical equations is developed which define and describe the relationships between the turbulent velocity, the Brunt-Väisälä frequency, the buoyancy length scale, the rate of dissipation of turbulent energy, the eddy diffusivity, and the time constant of the gravity wave generated, intermittent, decaying, coherent structures responsible for the scatterers detected by the IDI technique. It should be noted that the constants of proportionality are significantly different from the currently accepted values.

1. Introduction

S. J. Franke [private communication, 1997], following Booker *et al.* [1950], has questioned the validity of the identification of individual scatterers by the imaging Doppler interferometry (IDI) technique when the overall dimensions of the receiving interferometer are less than those of the transmitting antenna and has modeled this situation. He finds that the sum of the powers scattered by an ensemble of randomly moving scatterers distributed linearly across the transmitting beam width produces a linear phase across the receiving interferometer. Franke's model assumes scattering from a line of scatterers, and this has been shown by Briggs [1995] to produce just such a phase relationship. However, for randomly distributed, intermittent scatterers, such as those observed by the Middle Atmosphere Structure Associated Radiance (MAPSTAR) radar in the Arecibo Initiative on the Dynamics of the Atmosphere 1989 (AIDA'89) campaign, such a relationship is not observed. Using a model based on the observed scatterer properties, Roper [1998b] has demonstrated that the scatterer recovery technique of Brosnahan and Adams [1993] recovers

both the wind and turbulent velocity with acceptable error up to a wind velocity of some 60 m s^{-1} . The purpose of this paper is to compare the results of applying four analyses to the estimation of ϵ , the rate of dissipation of turbulent energy using MF radar data.

2. Structure Function Estimates of Turbulent Dissipation Rates

Batchelor [1953] presents a formulation of the velocity structure function which assumes only homogeneity and the Kolomogorov $-5/3$ power law. Roper and Brosnahan [1997] (hereinafter referred to as RB) have used this formulation to deduce the rate of dissipation of turbulent energy from the line of sight random velocities and separations of scatterers identified by the MAPSTAR imaging Doppler interferometer (IDI) MF radar during AIDA'89. In their formulation they chose to specify the velocity scale characterizing the turbulence as the velocity difference at which the velocity correlation coefficient fell to $1/e$, since this value, coupled with a guess of the time constant of the energy-bearing eddies as 100 s, yielded a rate of dissipation of turbulent energy not significantly different from that obtained using direct application of the structure function equation.

In this paper, an alternate approach to the rather unsatisfactory determination of the energy-bearing eddy scale L_0 is proposed. In attempting to determine

Copyright 2000 by the American Geophysical Union.

Paper number 1999RS002250.

0048-6604/00/1999RS002250\$11.00

must be over-estimates. Whether or not ϵ_ω (based on $L_\beta = L_\omega$) agrees with ϵ_r depends to first order on the Brunt-Väisälä frequency ω . Is the 20°N April monthly mean estimate of ω from Rees *et al.* [1990] even close at noon, the time at which the AIDA data used here were measured? Again we are reduced to uncertainty, a result typical of remotely sensed measurements of turbulence!

Weinstock's [1981] formula appears to overestimate ϵ . Weinstock concluded that anisotropy of the turbulence may account for differences in his applications to experimental data and should be taken into consideration in the calculation of radar-derived estimates. The question as to why Weinstock's theoretically derived equation provided a fit to estimates based on horizontal fluctuating velocities has not been answered. Any equation addressing buoyancy estimates should only be applied to the vertical fluctuating velocity, although all velocity components of the turbulence are correlated.

An attempt has been made to arrive at diffusivity formulations consistent with the derived buoyancy scale lengths and rate of dissipation of turbulent energy. The constant of proportionality (= 1.8) in (15) is 6 times larger than the generally accepted value of 0.33 which, being based on a critical Richardson number of $\frac{1}{4}$, is subject to the criticism detailed above.

In summary, the following set of self consistent equations has been developed:

Equation (4) $\epsilon_\beta = 0.16\sigma^2\omega$,

Equation (6a) $\epsilon_\omega = 0.1(u_\beta)^2\omega$,

Equation (15) $K_\epsilon = 1.8\epsilon\omega^{-2}$,

Equation (17) $K_\beta = 0.18(u_\beta)^2\omega^{-1}$,

Equation (18) $K_\omega = 0.3\sigma^2\omega^{-1}$.

These are also consistent with the length scales [Weinstock, 1978]

Equation (3) $L_\omega = (2\pi/0.62)\epsilon^{1/2}\omega^{-3/2}$,

and (RB)

Equation (5) $L_\beta = u_\beta\pi\omega^{-1}$,

and with the time constant of the intermittent, decaying coherent structures (scatterers) given by RB as

$$\tau = \pi\omega^{-1} \quad (19)$$

Note that these equations, while internally self consistent, are neither independent nor absolute. The equality of (15) and (17), for example, depends on (6a), while the constant of proportionality in equation (6a) depends on an equation of buoyancy length scales by RB which is based on a limited data set (some 200 AIDA'89 profile comparisons).

In conclusion, emphasis must again be placed on the fact that any estimates of the turbulent dissipation rate and accompanying atmospheric heating and diffusivity will be upper limits as long as the theory of stationary homogeneous turbulence is used to derive such estimates. Because of the difficulty in estimating the relative scatterer density, calculations of ϵ and K using the above formulae will also be upper limits.

The major problem in mesospheric studies is one of calibration. Rarely are measurements of the characteristics of this region available from more than one instrumental technique. The comparisons between the incoherent scatter and IDI radars made during AIDA'89 were complicated by the dissimilar volumes probed by the two instruments. The statement made by Hocking [1996] is echoed here, that more simultaneous common volume measurements (including instrumented rockets and rocket-released chemical trails) are essential to furthering this area of research.

Acknowledgments. This research is being supported by the Atmospheric Sciences (Aeronomy) Division of the National Science Foundation, under grant ATM-9728629.

References

- Adams, G. W., J. W. Brosnahan, and R. E. Johnson, Aspect sensitivity of 2.66-Mhz radar returns from the mesosphere, *Radio Sci.*, 24, 127-132, 1989.
- Batchelor, G.K., *The Theory of Homogeneous Turbulence*, 197pp., Cambridge Univ. Press, New York, 1953.
- Blix, T.A., E.V. Thrane, and O. Andreassen, In situ measurements of the fine scale structure and turbulence in the mesosphere and lower thermosphere by means of electrostatic positive ion probes, *J. Geophys. Res.*, 95, 5533-5548, 1990

FROM HOCKING, 1983 (JATP)

scales to 'go through' several cycles, and so there will be a larger r.m.s. velocity than for shorter data lengths. Further, the measured mean is more likely to be close to the 'true' mean when larger data samples are used.

Let the mean wind speed be \bar{v} . Let the data sample have temporal duration T . Then in this time T , a length $\bar{v}T$ of the atmosphere passes over the radar. It is constructive to examine the power spectrum produced from a radar data sequence recorded during the passage of this region of atmosphere, and to compare it to the structure function which would be measured for scales up to $\bar{v}T$.

As in equation (5), the structure function is defined by

$$\sigma_{||}^2(l) = \langle |v_{||}(x+l) - v_{||}(x)|^2 \rangle, \quad (14)$$

where $v_{||}(r)$ is the fluctuating velocity parallel to the mean velocity at position r , and l is the spatial lag in the direction parallel to the mean velocity. It is assumed that $v_{||}(r)$ is known as a function of r . Now let a region of horizontal size $L = \bar{v}T$ drift across the radar and assume that the turbulence remains (statistically) 'frozen' in the atmosphere (Taylor's hypothesis). Then the radar will measure a spectrum of velocities, with most energy at \bar{v} , and falling off in intensity either side of this peak. For argument's sake, take the probability distribution of horizontal fluctuating velocities to be Gaussian in form, with an r.m.s. velocity

$$v_H = \left[L^{-1} \int_0^L [v_{||}(l) - \bar{v}]^2 dl \right]^{1/2}. \quad (15)$$

Now assume that $v_{||}$ is a random function of position r (not true in reality, but an appropriate assumption in this case), and form the structure function (14). It can be shown that the distribution of velocity differences $[v_{||}(x+l) - v_{||}(x)]$ is also Gaussian, and

$$\sigma_{||}^2(L) = 2v_H^2. \quad (16)$$

(The assumption of a Gaussian distribution of velocities is in error, but it simplifies the discussion considerably, and does not drastically alter the conclusions.) But for turbulence

$$\sigma_{||}^2 = C_{v_H}^2 \epsilon^{2/3} l^{2/3}, \quad (17)$$

as in equation (5), and $C_{v_H}^2 \cong 2.0$ [see equation (5)]. Thus, using equation (16)

$$\epsilon \cong v_H^3/l. \quad (18)$$

Thus if it is possible to find a way to measure the r.m.s. horizontal velocity v_H , and if the mean wind speed of the atmosphere is known, as well as the data length of the sample, T , then equation (18) can be used to estimate ϵ . The parameter l should be taken as either $l = \bar{v}T$, or the approximate distance between the half-power points of

the polar diagram at the height of scatter—whichever parameter is the larger.

It is of interest to consider an alternative derivation of equation (18). The total mean square fluctuation of velocities v_H^2 could be rewritten as

$$1/2v_H^2 = \int_{k_1}^{\infty} E(k) dk + \int_{-\infty}^{-k_1} E(k) dk, \quad (19)$$

in a similar manner to equation (2). Here, k_1 represents the wavenumber of the longest scale which fits a full 'cycle' in the length $l = \bar{v}T$, viz.

$$k_1 = 2\pi/l.$$

Then the result

$$\epsilon \sim 3.5v_H^3/l, \quad (20)$$

is obtained, analogously to equation (7). Yet this result differs considerably from equation (18). Why? Equation (2) was valid because L_B was the largest scale. But in considering the case above, 2D turbulence was considered, in which case the largest scale is many times greater than the scales being dealt with. There was no effective 'cut-off' scale, and the scale $l = \bar{v}T$ is not the maximum scale contributing to the r.m.s. motion. It is the largest scale which makes a complete contribution, but larger scales exist and make some contribution to the r.m.s. velocity. So for the two-dimensional case described above, equation (19) is not valid. Rather, Fig. 4 describes the situation much better. The term $1/2v_H^2$ should equal the sum of the hatched and dotted areas there-in, and not just the hatched area. Scales larger than $k = 2\pi/(\bar{v}T)$ make a contribution, albeit a diminished one. Consequently equation (18) is correct, and equation (20) is in error for this case. Equation (18) is also valid for the case of 3D turbulence in which the resolution of the system is better than L_B . In this case, l should be taken as equal to the radar resolution, unless the data lengths become comparable to T_B .

It should also be pointed out that although the

Difference of a factor of 3!

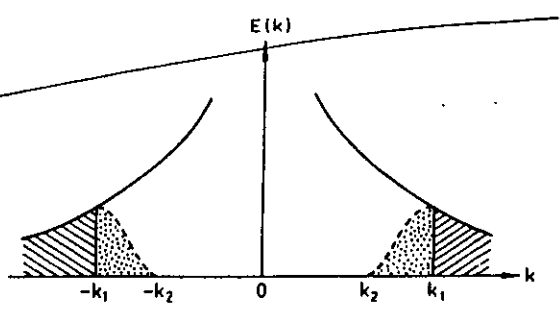


Fig. 4. Typical energy spectrum for turbulence (qualitative only). See text.

GRAVITY WAVES IN THE EARTH'S ATMOSPHERE.

We now turn our attention to
more "organized" dynamical
motions in the Earth's atmosphere.